PHILOSOPHICAL TRANSACTIONS OF THE ROYAL SOCIETY A MATHEMATICAL, PHYSICAL & ENGINEERING SCIENCES

The Elastic Strain Energy of Crystallographic Shear Planes in Reduced Tungsten Trioxide

E. Iguchi and R. J. D. Tilley

Phil. Trans. R. Soc. Lond. A 1977 **286**, 55-85
doi: 10.1098/rsta.1977.0110

THE ELASTIC STRAIN ENERGY OF CRYSTALLOGRAPHIC SHEAR PLANES IN REDUCED TUNGSTEN TRIOXIDE

BY E. IGUCHI† AND R. J. D. TILLEY
School of Materials Science, University of Bradford, Bradford BD7 1DP, Yorkshire, U.K.

(*Communicated by J. S. Anderson, F.R.S. – Received* 15 *July* 1976)

[Plates 1 and 2]

CONTENTS

Calculations of the elastic strain energy due to crystallographic shear (c.s.) planes lying upon {102}, {103} and {001} planes in reduced tungsten trioxide crystals have been made. The cases analysed in detail are for both isolated c.s. planes and for pairs of c.s. planes. These results are used to determine the elastic strain energy per unit volume for crystals containing ordered arrays of c.s. planes. It was found that the magnitude of the elastic strain energy was in the sequence {001} < {102} < {103} and that at relatively

† Present address: Department of Metallurgical Engineering, Yokohama National University, Ohka, Minamiku, Yokohama, 233 Japan.

Vol. 286. A 1332. 8 [Published 20 June 1977

small inter-c.s. spacings the curves of elastic strain energy against c.s. plane separation take the form of a series of peaks and valleys. These results are compared with experimental observations of c.s. plane spacings in substantially reduced crystals containing quasi-ordered arrays of c.s. planes and with observations of c.s. plane nucleation and growth in both slightly and more appreciably reduced crystals. It was found that the elastic strain energy plays a significant part in controlling the microstructure of c.s. plane arrays in such cases.

1. Introduction

It has been established for several years that if tungsten trioxide is reduced to compositions down to approximately $WO_{2.85}$ at temperatures in excess of about 1000 K the change in anion to cation stoichiometry is accounted for solely by the formation of crystallographic shear (c.s.) planes. If the degree of reduction is small, that is from WO_3 to approximately $WO_{2.95}$, the c.s. planes lie upon {102} planes† while if the composition is lower they lie upon {103} planes. When the reduction is achieved by reaction with certain lower valent metals, notably Ti, Nb, Ta or Mo, c.s. planes are also formed, although sometimes only over limited temperature as well as composition ranges. In these cases, the progression from {102} to {103} c.s. is usually observed to take place as the degree of reduction increases but the composition range over which each type occurs is in general different from that in the binary system. In addition, the Ti–W–O and Nb–W–O ternary oxides also make use of {104} and {001} c.s. planes to accommodate the oxygen loss, a feature not found in the binary system at all. More precise information on the crystal chemistry of these structures will be found in a number of recent review articles (Anderson 1972; Tilley 1972; Anderson & Tilley 1974; Tilley 1975; Ekström 1975.)

The observations outlined above have posed some interesting problems. As substantially reduced crystals often contain fairly well ordered arrays of c.s. planes with separations of 1.6–5.0 nm there is the question of the nature of the interactions between c.s. planes to account for. There have been a number of speculative discussions about the nature of these interaction forces and their origins (see, for example, Eyring & O'Keefe 1970, pp. 661–667) but only two publications have taken the matter further. Bursill & Hyde (1971) have proposed a qualitative form of inter-c.s. plane potential based upon experimental observations. Stoneham & Durham (1973) have made much more detailed quantitive calculations of the elastic strain energy of a pair of c.s. planes and ordered c.s. plane arrays. They chose, for this, {001} c.s. plane geometry in an ReO_3 structure and calculated the elastic strain energy by using a model which in essence is a *force* × *distance* one, in which the forces are those resulting from the introduction of a c.s. plane and the distance is the distortion of the structure due to the c.s. plane. Their results are of some interest. They found that the elastic strain energy for an array of c.s. planes was minimum for one particular inter-c.s. plane spacing and that for an isolated pair of c.s. planes the elastic strain energy was oscillatory and resulted in a series of maxima and minima. Although the model used by Stoneham & Durham is a simple one, there is reasonable agreement between their predictions of c.s. plane behaviour and the microstructure of crystals containing c.s. planes. To some extent the agreement is fortunate, as they compare their calculations, based on {001} c.s. in ReO_3, to experimental observations on the reduced titanium oxides, which chemically behave rather differently to the ReO_3 related tungsten oxides. Nevertheless, the results are in good enough agreement to suggest that calculations should be made for more realistic c.s. plane geometries and also compared more carefully with available experimental data corresponding to the c.s. plane models chosen.

† Throughout this paper the c.s. plane indices will be referred to an idealized cubic WO_3 cell of the $DO_9(ReO_3)$ type.

PHILOSOPHICAL TRANSACTIONS OF THE ROYAL SOCIETY A MATHEMATICAL, PHYSICAL & ENGINEERING SCIENCES

The sequence of c.s. planes found as reduction increases, from {102} to {103} and sometimes to {104} and {001} is also at first sight somewhat puzzling. The problem was discussed briefly by Stoneham & Durham (1973) who suggested that a change in c.s. plane type occurred if the total energies for two different types of c.s. plane crossed at some value of the composition of the crystal, but no details were given for real systems. The question was also considered in a recent paper (Tilley 1976) where it was suggested that {102} c.s. planes have the smallest formation energy and hence are nucleated preferentially in slightly reduced crystals. Thereafter, the formation energies are in the order {103} < {104} < {001}. It was also suggested that the precise composition at which one particular c.s. plane type changed to another was dependent upon both the formation energy and particularly the interaction energy between the c.s. planes.

The present report gives details of the quantitative calculation of the interaction energy between c.s. planes due to elastic strain of the surrounding crystal matrix. We have made these calculations in the first instance for the 3 major types of c.s. plane found, {102}, {103} and {001}. From the results we have attempted to explain some aspects of the microstructures of binary and ternary tungsten oxides containing c.s. planes, other aspects of which are to be covered in other communications.

2. Structural considerations

This section presents only a bare outline of the structural geometry of the c.s. containing binary and ternary tungsten oxides as it is known to date. Further information is to be found in the review articles already cited and more specific information will be introduced in the text where relevant.

Tungsten trioxide is built up of an infinite array of corner sharing WO_6 octahedra (figure 1*a*). The octahedra are distorted and the cations are somewhat off-centre giving rise to low symmetry structures, triclinic or monoclinic, which can be interconverted by temperature, grinding and impurities (Tanisaki 1960*a*, *b*; Roth & Waring 1966; Salje & Viswanathan 1975). The accepted stable room-temperature form is monoclinic, with cell parameters

$$a_0 = 0.7306\,\text{nm}, \quad b_0 = 0.7540\,\text{nm}, \quad c_0 = 0.7692\,\text{nm}, \quad \beta = 90.88°$$

(Loopstra & Boldrini 1966; Loopstra & Rietveld 1969). As the temperature increases, the distortion of the WO_6 octahedra changes and the symmetry passes from monoclinic through orthorhombic at about 600 K to tetragonal at about 1070 K (Salje & Viswanathan 1975; Ackermann & Sorrell 1970). The cubic form with the $ReO_3(DO_9)$ structure is never achieved in the binary system.

Reduction of WO_3 at temperatures higher than about 1000 K yields crystals which contain either {102} or {103} c.s. planes, depending upon composition. The idealized structures of each of these c.s. planes are shown in figure 1*b*, *c*. In general three microstructures have been observed in these samples. Slightly reduced material contains randomly distributed isolated {102} c.s. planes or small groups or clusters {102} c.s. planes. At greater degrees of reduction, fairly extensive volumes of reasonably well ordered {102} c.s. planes can result. If the ordering were complete the crystals would be members of a homologous series of oxides W_nO_{3n-1}, with the value of n depending upon the separation between the c.s. planes (figure 1*b*). More often, greater degrees of reduction lead to crystals containing quite well ordered arrays of {103} c.s. planes. These crystals, when perfectly ordered, belong to the homologous series of oxides W_nO_{3n-2}, and, again, the separation between the c.s. planes controls the value of n in the formula and hence the overall stoichiometry of the crystal (figure 1*c*).

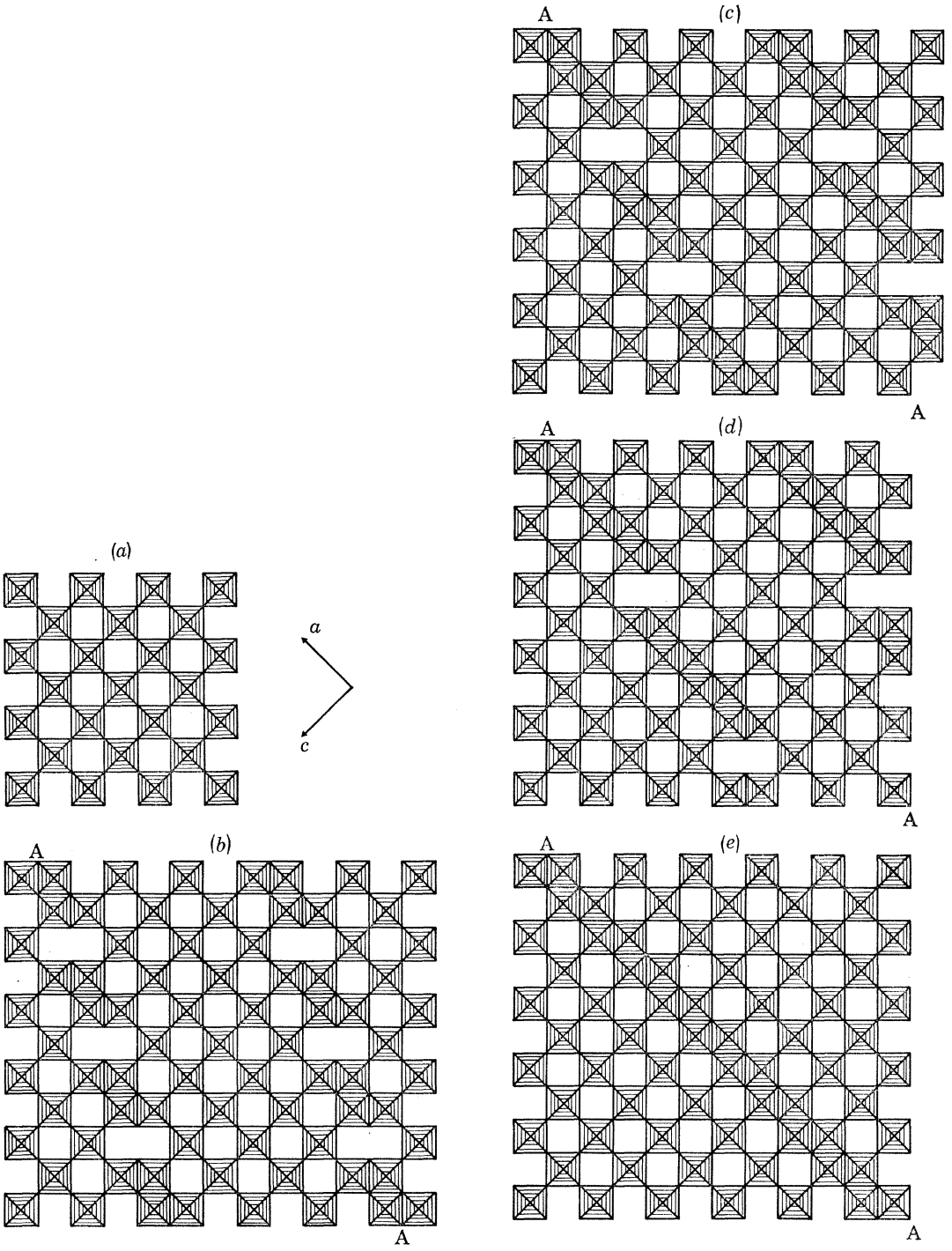

FIGURE 1. Idealized representations of (*a*) WO_3; (*b*) $W_{11}O_{32}$, an oxide containing {102} c.s. planes; (*c*) $W_{15}O_{43}$, an oxide containing {103} c.s. planes; (*d*) $W_{19}O_{54}$, an oxide containing {104} c.s. planes; (*e*) a single {001} c.s. plane. In (*b*) (*c*) and (*d*) the value of n in the oxide formulae W_nO_{3n-1}, W_nO_{3n-2} or W_nO_{3n-3} is given by the number of linked octahedra in the direction *AA*, and in (*e*) by the number of octahedra normal to the c.s. planes.

PHILOSOPHICAL TRANSACTIONS OF THE ROYAL SOCIETY A MATHEMATICAL, PHYSICAL & ENGINEERING SCIENCES

Reduction of WO_3 with other metals only rarely produces c.s. phases. When this is the case, the same trend of formation is followed, but the range of composition over which the {102} and {103} c.s. planes are stable varies considerably. For example in the ternary Mo–W–O system, the formation of {103} c.s. planes is suppressed so that only {102} c.s. planes are observed. In the Ta–W–O system, on the other hand the {102} c.s. phases are extinguished almost completely and a wide range of compositions is accommodated by {103} c.s. planes. This, however, only holds good at temperatures above about 1500 K, and below this temperature quite different structures seem to be stable (Ekström 1975; Ekström & Tilley 1976).

The case with Nb and Ti is different again. In these ternary systems, although the {102} and {103} c.s. sequence is adhered to, {001} c.s. planes seem to be favoured and form in preference to extended {102} or {103} ranges. c.s. planes with indices between {103} and {001} also form, particularly in the Nb_2O_5-WO_3 oxides, where well ordered {104} c.s. phases have been recorded. (Allpress 1972; Bursill & Hyde 1972; Ekström & Tilley 1974). Figure 1*d*, *e* show the idealized structures of these c.s. planes. As with the {102} and {103} c.s. planes, ordered arrays of {104} and {001} c.s. planes give rise to homologous series of oxides with formulae $(M, W)_n O_{3n-3}$ and $(M, W)_n O_{3n-1}$ respectively, and, as before, the value of n in the formula is closely related to the c.s. plane separation.

The microstructures of the ternary oxides containing c.s. planes are not so well characterized as those formed in the binary system, but it is known that well ordered arrays of {104} and {001} c.s. planes do occur and also disordered intergrowths between {104} and {001} c.s. planes. Well ordered c.s. planes with higher indices, {105}, {106} and so on, have not been reported in the literature, with one exception (Gadó 1974) but may occur under experimental conditions not yet investigated.

The real structures of almost all of these phases are unknown, although there are some X-ray studies on the {102} and {103} c.s. phases in the literature (references to which are contained in the review articles cited in the Introduction.) In general we can say that the metal oxygen octahedra will be distorted to varying degrees in these materials, and that the distortions are likely to be temperature sensitive, as in WO_3 itself.

3. Thermodynamic considerations

The general trend of c.s. plane indices passing from {102} to {103} and ultimately {001} has been considered in a preceding publication (Tilley 1976). It was suggested that the reduction of a WO_3 crystal could be expressed formally by the equation

$$WO_3\,(c) \rightarrow WO_{3-x}\,(c, c.s.) + \tfrac{1}{2}xO_2\,(g)$$

and that the free energy of the reduced crystal, WO_3 (c, c.s.) containing c.s. planes could be expressed as

$$G\,(N, N_d, T) = G_0\,(N) + G_d\,(N, N_d) + G_i\,(N_d). \qquad (1)$$

In this equation G_0 is the free energy of the original (perfect) WO_3 crystal before reduction and which contains N tungsten atoms, G_d is the free energy of the N_d c.s. planes introduced as a result of the reduction and G_i is a free energy contribution resulting from all the interactions between the c.s. planes and their surroundings. In such a formalism, G_0 is expected to be dominant while G_d and G_i are responsible for the equilibrium microstructures to be found in the crystals. From this point of view, G_d is analogous to a defect formation energy and G_i to a defect interaction energy.

The sequence of c.s. planes observed on reduction of WO_3 indicates that the G_d term for {102} c.s. plane formation is lowest, and then we obtain, in order {103}, {104} ... {10m} ... {001}. This will then set a pattern for the reduction behaviour. However the G_i term will be important in controlling the composition at which one c.s. plane type gives way to another. Although a knowledge of the formation energies is able to give a general reaction scheme for the course of reduction, real systems are going to behave in a way which strongly reflects the nature of the interactions between the c.s. planes and their surroundings. It is therefore of some interest to try to evaluate these energy terms theoretically.

The interaction terms can be divided up into chemical and mechanical parts. The chemical factors involve the preference of ions for sites within the c.s. plane or within the matrix, the tendency for the ions to partake in cation–cation and cation–anion–cation bonding within the c.s. plane and the extent to which the outer electrons on the cations are delocalized within the structure. At present these effects are difficult to treat in anything other than a qualitative fashion. The mechanical factors are more readily assessed. They can be thought of as arising principally from elastic strain of the matrix by the c.s. plane and electrostatic interactions between the c.s. planes and the matrix or each other. We have made quantitative calculations of the magnitude of both the elastic strain interaction energy and the electrostatic interaction energy for a number of c.s. plane geometries. In this report we present the results of the elastic strain interaction energy calculations for {102}, {103} and {001} c.s. plane geometries, while a future communication will give details of the electrostatic interaction energies.

The elastic strain energy term will take the form of an internal energy function, U, so that we can assume that when one c.s. plane is introduced into a perfect WO_3 crystal, the increase in internal energy due to elastic strain will be

$$U_1 = (U_s)_{self} + (U_s)_1. \tag{2}$$

$(U_s)_{self}$ represents the elastic strain energy of the c.s. plane itself, that is, the edge-shared units of WO_6 octahedra characterizing the plane of collapse of the matrix and $(U_s)_1$ is the elastic strain of the matrix surrounding the c.s. plane. These components are shown schematically in figure 2. Similarly, we assume that when a pair of c.s. planes, *1* and *2*, are introduced into a perfect crystal, the increase in the internal energy due to elastic strain, U_2, can be expressed by the following equation

$$U_2 = 2(U_s)_{self} + (U_s)_1 + (U_s)_2, \tag{3}$$

where $(U_s)_2$ is the increase in the elastic strain energy of all the atoms between the two c.s. planes. From equations (2) and (3) it is readily shown that the energy difference between a pair of c.s. planes and two isolated c.s. planes is given by equation (4).

$$\Delta U_2 = U_2 - 2U_1 = (U_s)_2 - (U_s)_1. \tag{4}$$

From this it follows that the internal energy difference between a cluster of n c.s. planes and n isolated c.s. planes, ΔU_n, can be written as

$$\Delta U_n = (n-1)\,[(U_s)_2 - (U_s)_1]. \tag{5}$$

The term $(U_s)_{self}$ has been formally considered to be part of the G_d function in equation (1) and will not be evaluated. In this report we have derived theoretical expressions for the terms $(U_s)_1$ and $(U_s)_2$ and have evaluated them numerically for a number of c.s. plane geometries. It should be noted here that this equation only holds provided that interactions between other than

nearest neighbour c.s. planes are neglected. The equation (5) therefore represents an approximation which should be born in mind in later discussions. The most important shortcoming of this approximation is that the interaction energy for a pair of c.s. planes in the middle of a cluster

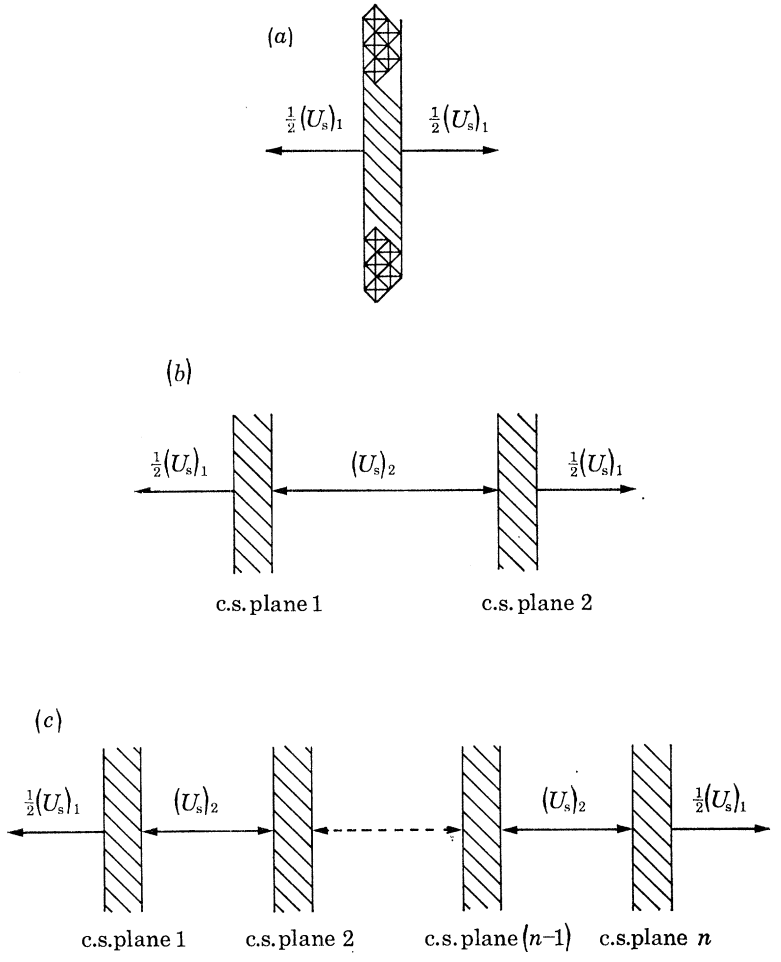

FIGURE 2. Schematic representation of the components of the total elastic strain energy of crystals containing c.s. planes; (*a*) isolated c.s. plane; (*b*) a pair of c.s. planes; (*c*) *n* c.s. planes (see text for details).

is the same as the interaction energy between a pair of c.s. planes near the edge of the cluster, and moreover, this interaction energy will not change as the size of the cluster varies. This is unlikely to be true in practice and experimental evidence for clusters of c.s. planes in reduced rutile (Bursill & Hyde 1971) shows it not to be so in that system. The theoretical treatment of Stoneham & Durham (1973) does include a consideration of these next nearest neighbour interactions, and their results are in agreement with the experimental evidence for rutile. However, in the reduced tungsten oxides the approximation does not seem to be so severe and the available experimental evidence suggests that a neglect of the next-nearest neighbour interactions are not so important (see § 6 (*c*) and figure 13).

It is difficult to make an accurate assessment of the entropy contribution to the free energy term G_1. While it is possible to consider that the configurational entropy of isolated c.s. planes or of disordered arrays of c.s. planes in macroscopic crystals to be negligible, certainly in comparison with the configurational entropy terms associated with point defect populations, for

example, the contribution due to vibrational entropy is not readily evaluated and may be quite significant. A consideration of the structure of c.s. planes compared to that of the parent WO_3 structure shows them to be much more densely packed with atoms. This is true of the oxygen atoms which fill some of the empty anion positions in the WO_3 structure as well as the cations, which also fill normally unoccupied but available cation sites. In the geometrical sense this is equivalent to the intergrowth of thin lamellae of an oxide of stoichiometry WO_2 with the anatase structure in the parent matrix. The vibrational freedom of the c.s. plane is therefore likely to be more restricted than in the WO_3 parent and to tend towards that of WO_2 which, it should be remembered, has the rutile structure, not the anatase structure. The contribution of the vibrational terms will increase as the c.s. plane density increases, but it is difficult to allot a contribution per c.s. plane as c.s. plane interactions will certainly modify the vibrational properties of the crystals. Because of this we cannot approximate the elastic strain energy terms to free energies. However it is not unreasonable to equate $(U_s)_1$, $(U_s)_2$ and ΔU_n to enthalpies and to suppose that they will make a substantial contribution to G_i, particularly at lower temperatures. In order to determine just how important this contribution is, the absolute magnitude of the energies must be obtained and compared with the electrostatic energies already referred to. Such calculations are at present in progress and will be reported in the future (Iguchi, to be published).

4. Theory

To obtain the strain energies $(U_s)_1$ and $(U_s)_2$ we have used classical elasticity theory. This approach is somewhat different to the method employed by Stoneham & Durham (1973), but leads to related energy terms. In essence the method we have used is as follows. First we assume that the c.s. planes are a source of forces acting upon the surrounding matrix. In the simplest case we can treat these forces as arising from ionic interactions and this will be taken as the case in the present report. More sophisticated models for the generation of the forces can also be chosen, of course. With a knowledge of the forces arising in the c.s. plane (both in magnitude and direction) we can determine the displacement of the ions surrounding the c.s. plane. The displacements which cause a deformation of the crystal matrix are readily converted into strains, by differentiation with respect to direction, to obtain the strain components e_{xx}, e_{yy}, etc. In our treatment these components contain a displacement term as well as a term containing the force responsible for the displacement, and we have a result analogous to that of Stoneham & Durham (1973) namely an elastic strain energy equation containing '*force* × *distance*' terms, but presented in an alternative fashion. The strain components are readily converted into absolute strain energies by, in essence, multiplication by the known elastic constants of the material, the Lamé constant λ and the shear modulus μ. The individual steps in the theory are now given in detail.

In order to simplify the theoretical treatment we have made the following assumptions: (i) The crystal structure of WO_3 is of the ideal cubic $ReO_3(DO_9)$ type, (ii) the crystal can be treated as an isotropic continuum except in the region of the c.s. plane which is considered as containing discrete ions. The strain energies can then be calculated by the use of linear elasticity theory. In order to simplify this task as much as possible a set of axes has been chosen which allows the equations for the strain energy, equations (6)–(17), to be expressed in as concise a fashion as possible. These axes, which are shown on figures 3 and 4, have the x-axis parallel to the crystallographic direction $(10\bar{1})$, the y-axis parallel to the crystallographic direction (101) and the z-axis parallel to the crystallographic direction (010). It should be noted that these

axes are employed only in the calculations, and all features of crystallographic relevance, such as c.s. plane indices or directions are referred to the conventional crystallographic unit cell and axes shown on figure 1.

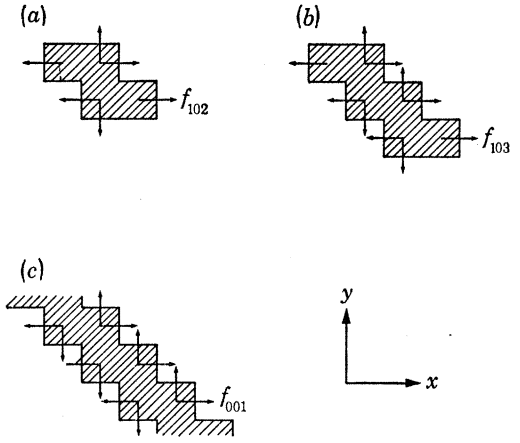

FIGURE 3. The direction of the forces assumed to be present within a c.s. plane and which result in elastic strain energy of the surrounding matrix, (*a*) {102} c.s. plane; (*b*) {103} c.s. plane, (*c*) {001} c.s. plane. The axes are those used in the calculations and not the crystallographic axes.

First we consider the forces responsible for the strain in the crystal. From figure 1 it can be seen that in the c.s. planes, the cations in the mirror plane (010) and the anions in the planes above and below them are brought closer together than in the parent WO_3-like matrix. If we assume an ionic structure for the c.s. plane the major forces will be ones of repulsion between the cations in the (010) plane and between the anions above and below them. It is a relatively straightforward matter to estimate these repulsive forces f_{102}, f_{103} and f_{001}. This is illustrated in appendix A. The directions of such forces are shown in figure 3. These forces, which are undoubtedly large, are not explicitly calculated in this report, but are assimilated into the general term G_d in equation (1).

(*a*) *Isolated c.s. planes*, $(U_s)_1$

As mentioned above, elasticity theory for an isotropic continuum is now used to obtain the strain energy of the ions near the c.s. plane due to the forces f_{102}, f_{103} and f_{001} just described assuming $f_{102} \simeq f_{103} \simeq f_{001} = f$. In order to define the coordination of each unit a reference position has been chosen as shown in figure 4 so that the coordination of the ith unit is given by the coordinates (X_1, Y_1, Z_1). The unit of length used along the x, y and z axes is the length of an idealized WO_6 octahedron edge, $a/\sqrt{2}$, where a is the unit cell edge of the idealized cubic WO_3, equal to the octahedron diagonal length. By applying the theory (see appendix B) each component of the displacement of the Ith ion at (X_I, Y_I, Z_I) caused by the point forces in the ith unit of a c.s. plane $(u_1)_1$ $(u_2)_1$ and $(u_3)_1$ is readily obtained. To illustrate the procedure, we outline how to obtain the x component of the displacement, $(U_1)_1$ for a {103} c.s. plane, which is given by:

$$\begin{aligned}(u_1)_1 = {} & (u_{11})_{x,y,z} \\ & + (u_{11})_{x+1,y-1,z} + (u_{12})_{x+1,y-1,z} \\ & + (u_{11})_{x+2,y-2,z} + (u_{12})_{x+2,y-2,z} \\ & - (u_{11})_{x+1,y,z} - (u_{12})_{x+1,y,z} \\ & - (u_{11})_{x+2,y-1,z} - (u_{12})_{x+2,y-1,z} \\ & - (u_{11})_{x+3,y-2,z}. \end{aligned} \tag{6}$$

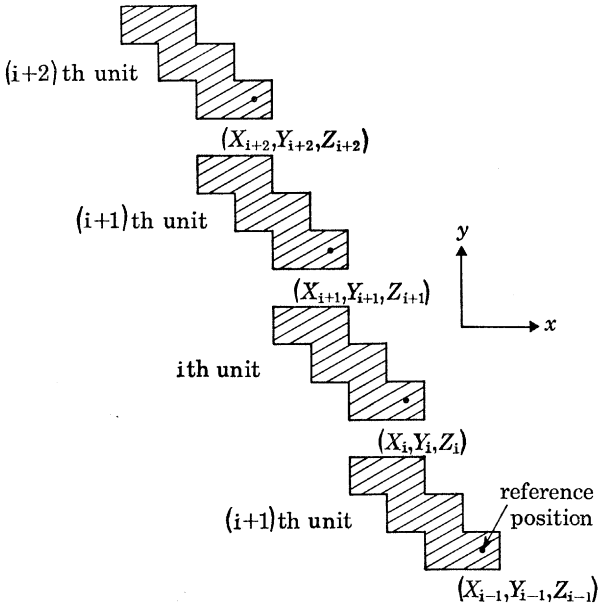

FIGURE 4. Notation for locating the positions of the units comprising a {103} c.s. plane. The axes are those used in the calculations and not the crystallographic axes.

In equation (6), $(u_{hk})_{x,y,z} = u_{hk}(\boldsymbol{r})$ and $\boldsymbol{r} = (X_I - X_1)\boldsymbol{i} + (Y_I - Y_1)\boldsymbol{j} + (Z_I - Z_1)\boldsymbol{k} = x\boldsymbol{i} + y\boldsymbol{j} + z\boldsymbol{k}$, where $\boldsymbol{i}$, $\boldsymbol{j}$ and $\boldsymbol{k}$ are the unit vectors along the x, y and z axis. Therefore, equation (6) can be rewritten to yield equation (7).

$$
\begin{aligned}
(u_1)_1 = {} & (A-B)\left\{\sum_{l=1}^{3}(1/|\boldsymbol{r}_l|) - \sum_{l=4}^{6}(1/|\boldsymbol{r}_l|)\right\} \\
& + B\left\{\sum_{l=1}^{3}(x+1-1)^2/|\boldsymbol{r}_l|^3 - \sum_{l=4}^{6}(x+1-3)^2/|\boldsymbol{r}_l|^3\right\} \\
& + B\left\{\sum_{l=2}^{3}(x+1-1)(y-1+1)/|\boldsymbol{r}_l|^3 - \sum_{l=4}^{5}(x+1-3)(y-1+4)/|\boldsymbol{r}_l|^3\right\}, \qquad (7)
\end{aligned}
$$

where

$$
\begin{aligned}
A &= 2f_{(103)}/8\pi\mu, \\
B &= (f_{(103)}/8\pi\mu)(\lambda+\mu)/(\lambda+2\mu), \\
\boldsymbol{r}_l &= (x+1-1)\boldsymbol{i} + (y-1+1)\boldsymbol{j} + z\boldsymbol{k} \quad \text{for} \quad l = 1, 2, 3, \\
\boldsymbol{r}_l &= (x+1-3)\boldsymbol{i} + (y-1+4)\boldsymbol{j} + z\boldsymbol{k} \quad \text{for} \quad l = 4, 5, 6.
\end{aligned}
$$

In a similar way, $(u_2)_1$ and $(u_3)_1$ can be obtained.

The kl component of the strain, e_{kl}, is related to the components of the displacement by the following equation:

$$e_{kl} = (\alpha u_k/\alpha x_l + \alpha u_l/\alpha x_k)/2. \qquad (8)$$

We can now obtain the strain component of the Ith ion at (X_I, Y_I, Z_I) due to the ith unit in the c.s. plane $(e_{11})_1$, $(e_{22})_1$, $(e_{33})_1$, $(e_{12})_1$, $(e_{23})_1$, $(e_{31})_1$ by using equations in appendix B and equation (8). As an example, we show $(e_{11})_1$ which is given in equations (9), (10).

$$(e_{11})_1 = \sum_{l=1}^{3} (\alpha u_{11}/\alpha x)_{x+l-1,\,y-l+1,\,z} + \sum_{l=2}^{3} (\alpha u_{12}/\alpha x)_{x+l-1,\,y-l+1,\,z} - \sum_{l=4}^{6} (\alpha u_{11}/\alpha x)_{x+l-3,\,y-l+4,\,z} - \sum_{l=4}^{5} (\alpha u_{12}/\alpha x)_{x+l-3,\,y-l+4,\,z} \tag{9}$$

$$\textit{i.e. } (e_{11})_1 = (-A+3B)\left\{\sum_{l=1}^{3} (x+l-1)/|r_l|^3 - \sum_{l=4}^{6} (x+l-3)/|r_l|^3\right\} + B\sum_{l=2}^{3}\{(y-l+1)/|r_l|^3 - 3(x+l-1)^2(x+y)/|r_l|^5\} - B\sum_{l=4}^{5}\{(y-l+4)/|r_l|^3 - 3(x+l-3)^2(x+y+1)/|r_l|^5\} - 3B\{x^3/|r_7|^5 - (x+3)^3/|r_6|^5\}, \tag{10}$$

where $(\alpha u_{hk}/\alpha x)_{x,y,z}$ indicates $\alpha(u_{hk})_{x,y,z}/\alpha x$ and so on. Therefore, the kl component of the strain of the ion I at (X_I, Y_I, Z_I) caused by the c.s. plane, $(e_{kl})_I$, is given by

$$(e_{kl}) = \sum_i (e_{kl})_1, \tag{11}$$

where $\sum_i$ indicates the summation of the strain caused by every unit in the c.s. plane.

In an isotropic continuum, the strain energy density ω has the form

$$\omega = (\lambda+2\mu)\tfrac{1}{2}(e_{11}+e_{22}+e_{33})^2 + 2\mu(e_{12}^2+e_{23}^2+e_{31}^2-e_{11}e_{22}-e_{22}e_{33}-e_{33}e_{11}). \tag{12}$$

Then, the strain energy of the Ith ion with ionic radius r_I due to the c.s. plane, $(E_s)_I$, can be given by equation (13):

$$(E_s)_I = (4\pi/3)(r_I)^3[\tfrac{1}{2}(\lambda+2\mu)\{(e_{11})_I+(e_{22})_I+(e_{33})_I\}^2 + 2\mu\{(e_{12})_I^2+(e_{23})_I^2+(e_{31})_I^2-(e_{11})_I(e_{22})_I(e_{22})_I(e_{33})_I-(e_{33})_I(e_{11})_I\}]. \tag{13}$$

Therefore, $(U_s)_1$ has the form

$$(U_s)_1 = \sum_I (E_s)_I, \tag{14}$$

where $\sum_I$ indicates the summation of the strain energies of all ions in the crystal except the ions inside the c.s. plane.

The value of $(U_s)_1$ due to a {102} or {001} c.s. plane can be obtained by similar methods.

(*b*) *Paired c.s. planes*, $(U_s)_2$

The jth component of the displacement of the I ion at (X_I, Y_I, Z_I) between the c.s. planes *1* and *2*, $(u_j)_I$, is given by equation (15).

$$(u_j)_1 = \sum_i^1 (u_j)_i + \sum_{i'}^2 (u_j)_{i'}, \tag{15}$$

where $(u_j)_i$ is the jth component of the displacement of the Ith ion caused by the ith unit in c.s. plane *1* and $(u_j)_{i'}$ by the ith unit in c.s. plane *2*. The notation $\sum_i^1$ means the summation of the jth component of the displacement due to all units in c.s. plane *1* and $\sum_{i'}^2$ a similar summation over all units in c.s. plane *2*.

PHILOSOPHICAL TRANSACTIONS OF THE ROYAL SOCIETY A MATHEMATICAL, PHYSICAL & ENGINEERING SCIENCES

Then, the kl component of the strain of the Ith ion has the form,

$$(e_{kl})_I = \sum_{i}^{1} \tfrac{1}{2}\{\alpha(u_k)_i/\alpha(x_l)_i + \alpha(u_l)_i/\alpha(x_k)_i\} + \sum_{i'}^{2} \tfrac{1}{2}\{\alpha(u_k)_{i'}/\alpha(x_l)_{i'} + \alpha(u_l)_{i'}/\alpha(x_k)_{i'}\}$$
$$= \sum_{i}^{1} (e_{kl})_{i'} + \sum_{i'}^{2} (e_{kl})_{i'} \qquad (16)$$

where $(x_l)_i = (X_l)_I - (X_l)_i$ and $(x_l)_{i'} = (X_l)_I - (X_l)_{i'}$ and the coordinates (X_l, Y_l, Z_l) and $(X_{l'}, Y_{l'}, Z_{l'})$ are the reference positions of the ith unit in c.s. plane *1* and the ith unit in c.s. plane *2*.

We can obtain $(U_s)_2$ by substituting equation (16) into equation (12):

$$(U_s)_2 = \sum_{I}^{1,2} (4\pi/3)(r_I)^3[\tfrac{1}{2}(\lambda + 2\mu)\{(e_{11})_I + (e_{22})_I + (e_{33})_I\}^2$$
$$+ 2\mu\{(e_{12})_I^2 + (e_{23})_I^2 + (e_{31})_I^2 - (e_{11})_I(e_{22})_I - (e_{22})_I(e_{33})_I - (e_{33})_I(e_{11})_I\}], \qquad (17)$$

where $\sum_{I}^{1,2}$ indicates the summation of the strain energies of all ions between the c.s. planes *1* and *2*.

As before, an analogous treatment allows $(U_s)_2$ for {102} and {001} c.s. planes to be derived.

5. Calculations

In order to calculate the strain energies, $(U_s)_1$ and $(U_s)_2$, due to {102} {103} and {001} c.s planes introduced into a crystal the ratios of the elastic constants of the crystal and also the ratio of the ionic radii of the ions must be known. Unfortunately the elastic constants of WO_3 have not yet been determined so we have used the same ratios of the elastic constants as Stoneham & Durham (1973), i.e.

$$C_{11}:C_{12}:C_{44} = 16:7:5.$$

In addition, the following ionic radii for O^{2-} ions and W^{6+} ions were used in this calculation (Shannon & Prewitt 1969)

r_0 (the ionic radius of O^{2-}) = 0.140 nm,

r_w (the ionic radius of W^{6+}) = 0.060 nm.

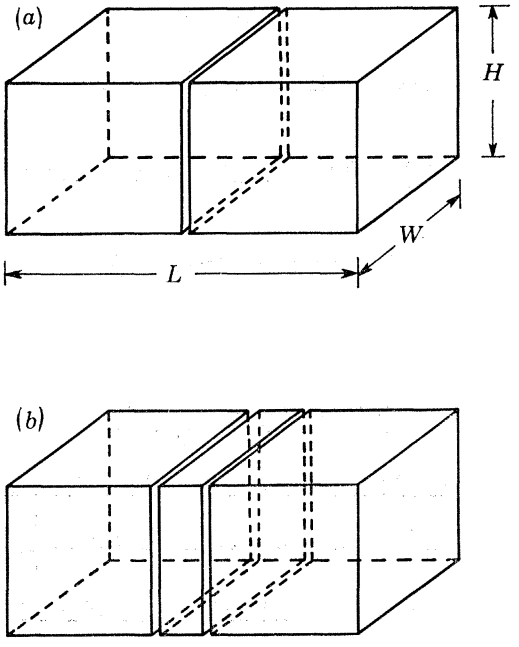

Figure 5. Schematic representation of a crystal containing (*a*) a single c.s. plane and (*b*) a pair of c.s. planes.

The strain energies, $(U_s)_1$ and $(U_s)_2$, are defined in this report in the following way. One c.s. plane is introduced into a single crystal (height $H \times$ width L) as shown in figure 5 and this c.s. plane strains all ions in the crystal. The summation of the strain energy of each ion in the crystal due to this c.s. plane is divided by the cross-section of the crystal, $H \times W$, and this energy per unit area is defined as $(U_s)_1$. Similarly, when two c.s. planes are introduced into the crystal, the summation of the strain energies of all ions between these two c.s. planes is also divided by the cross sectional area and it is this value that is defined as $(U_s)_2$. The values of the height, width and especially the length should be large in order to make the calculated values valid.

(*a*) *Isolated c.s. planes*, $(U_s)_1$

In order to evaluate $(U_s)_1$, one should ideally calculate the strains of all ions in the crystal, but this is clearly impractical. Thus in this calculation of the strain we consider only those ions which lie between the c.s. plane and a position which is separated from the centre line in the unit by a distance of $21.5a$, where a is the length of the diagonal of a tungsten–oxygen octahedron, approximately 0.38 nm. It also follows from eq. (14) that the strain of each ion should ideally be the summation of the strains due to all of the units in the c.s. plane. This calculation is also impractical, so we have chosen to sum only the strains due to 31×35 units, in the case of a {102} c.s. plane, 21×41 units in the case of a {103} c.s. plane and 85×41 units in the case of an {001} c.s. plane. The units which give the largest strain are, as expected, in the centres of these

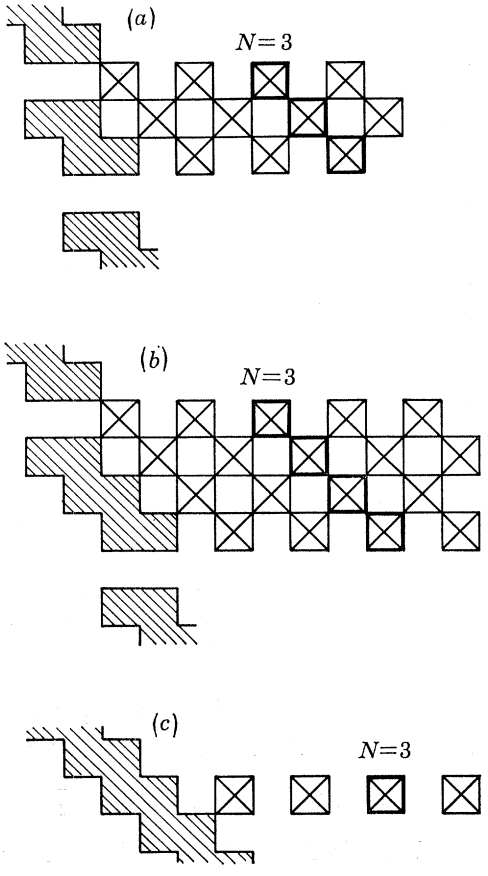

FIGURE 6. Notation for indicating the value of N used in the calculations.

blocks of units and it was found that the absolute value of the ratio of the strain due to a unit in the boundary to the strain due to a unit in the centre was less than 0.01. By using these conditions, the strain energy of each ion was calculated from equations (10) and (13), and then $(U_s)_1$ obtained using equation (14). The steps in this calculation are outlined below.

In the case of a {102} c.s. plane there are three octahedra parallel to each unit which have their centres at a distance of $(2N+\frac{1}{2})a$, from the centre line in each unit, where N is a positive integer (see figure 6). The average value of the strain energies of these three octahedra obtained according to equation (14), $E_s(N)$, is related to $(U_s)_1$ by the following equation,

$$(U_s)_1 \propto \sum_{N=1}^{\infty} E_s(N). \tag{18}$$

In the case of a {103} c.s. plane, the method of obtaining $(U_s)_1$ is almost the same, but $E_s(N)$ indicates the average value of the strain energies of four octahedra, because each unit in a {103} c.s. plane has four octahedra at a distance of $(2N+\frac{1}{2})a$ from the centre line in the unit. As a {001} c.s. plane has only one octahedron at the distance of $(2N+\frac{1}{2})a$, then $E_s(N)$ indicates the strain energy of this octahedron (see figure 6).

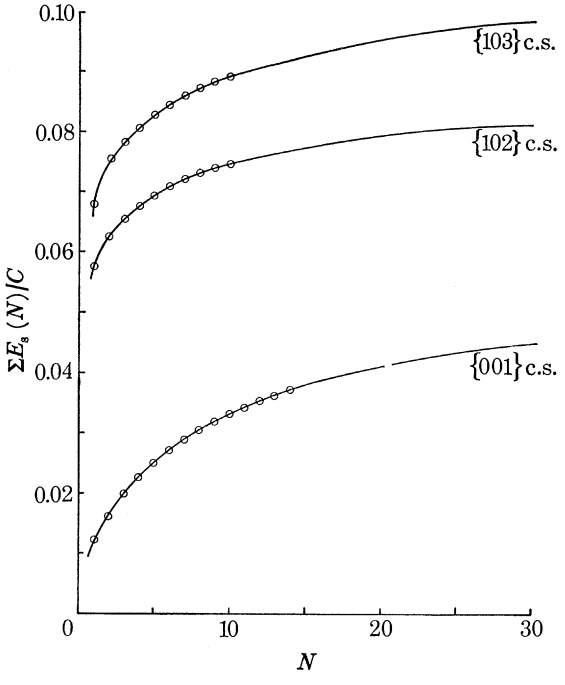

FIGURE 7. The elastic strain energy for single {102}, {103} and {001} c.s. planes in an idealized WO_3 matrix, $\Sigma E_s(N)/C$, as a function of N, the distance from the c.s. plane. The curves have been extrapolated to yield values of the elastic strain energy $\Sigma E_s(N)/C$ as N becomes large.

The results of the calculations are presented in figure 7, where the values of $\Sigma E_s(N)$ are plotted as a function of N. In these figures the vertical axis indicates $\Sigma E_s(N)/C$ where

$$C = [(\lambda + 2\mu)(f/8\pi\mu)^2(4\pi r_0^3/3)]$$

and the horizontal axis shows N. Table 1 contains the data used in constructing figure 7. By considering the symmetry of the c.s. plane and using the extrapolated values of $\Sigma E_s(N)$ from

figure 7 the values of $(U_s)_1$ for {102} {103} and {001} c.s. planes are found to be

$$[(U_s)_1]_{102} = (3/\sqrt{5}\,a)\,(1/a)\,(1/a)2\sum_{N=1}^{\infty} E_s(N)$$
$$\simeq 0.2180C/a^2, \tag{19a}$$

$$[(U_s)_1]_{103} = (4/\sqrt{10}\,a)\,(1/a)2\sum_{N=1}^{\infty} E_s(N)$$
$$\simeq 0.2490\,C/a^2, \tag{19b}$$

and

$$[(U_s)_1]_{001} = (1/a)\,(1/a)2\sum_{N=1}^{\infty} E_s(N)$$
$$\simeq 0.0900\,C/a^2. \tag{19c}$$

TABLE 1. THE ELASTIC STRAIN ENERGY OF ISOLATED C.S. PLANES

	{102} c.s.		{103} c.s.		{001} c.s.	
N	$E_s(N)/C$	$(1/C)\,\Sigma E_s(N)$	$E_s(N)/C$	$(1/C)\,\Sigma E_s(N)$	$E_s(N)/C$	$(1/C)\,\Sigma E_s(N)$
1	0.057178	0.057178	0.067919	0.067919	0.012344	0.012344
2	0.005412	0.062590	0.007646	0.075560	0.003120	0.015464
3	0.002804	0.065394	0.002829	0.078389	0.004332	0.019796
4	0.002305	0.067699	0.002381	0.080770	0.002725	0.022521
5	0.001832	0.069531	0.002050	0.082820	0.002417	0.024938
6	0.001444	0.070975	0.001733	0.084553	0.002108	0.027046
7	0.001158	0.072133	0.001458	0.086011	0.001819	0.028865
8	0.000966	0.073099	0.001238	0.087249	0.001566	0.030431
9	0.000848	0.073947	0.001073	0.088322	0.001360	0.031791
10	0.000782	0.074729	0.000955	0.089277	0.001211	0.033002
11					0.001102	0.034104
12					0.001048	0.035152
13					0.001037	0.036189
14					0.001063	0.037252
∞		~ 0.0812†		~ 0.0984†		~ 0.0450†

† These values are estimated by extrapolation to high N values as shown in figure 7, and are for one side of the c.s. plane only.

(*b*) *Paired c.s. planes* $(U_s)_2$

Next, we calculate the value of $(U_s)_2$. As shown in figure 5 two c.s. planes are to be introduced into a large single crystal. The composition of the crystal between these c.s. planes can be considered to be given by the formula W_nO_{3n-1} in the case of {102} and {001} c.s. planes and by W_nO_{3n-2} in the case of {103} c.s. planes, where n is a measure of the separation between the c.s. planes (see figure 1). The value of $(U_s)_2$, which depends upon n, was calculated by applying equation (17). The results are shown in figure 8, where the vertical axis shows $(U_s)_2a^2/C$. The numerical data are also given in table 2.

It can be seen that as n or the composition increases towards WO_3 broadly speaking the values of $(U_s)_2$ increase. However, in the lower part of the composition range the curve is not a smooth one but consists of a series of peaks and valleys.

TABLE 2. THE ELASTIC STRAIN ENERGY BETWEEN A PAIR OF C.S. PLANES, $(U_s)_2 a^2/C$, AS A FUNCTION OF THE SPACING BETWEEN THEM, d_x

	{102} c.s.			{103} c.s.			{001} c.s.		
n	x in WO_x	d_x(nm)	$(U_s)_2 a^2/C$	x in WO_x	d_x(nm)	$(U_s)_2 a^2/C$	x in WO_x	d_x(nm)	$(U_s)_2 a^2/C$
3							2.6667	0.950	0.048908
4							2.7500	1.330	0.042546
5							2.8000	1.710	0.059066
6	2.8333	0.935	0.194028				2.8333	2.090	0.066794
7	2.8571	1.105	0.155766				2.8571	2.470	0.080286
8	2.8750	1.275	0.164738				2.8750	2.850	0.084544
9	2.8889	1.445	0.181256	2.7778	0.960	0.210002	2.8889	3.230	0.091302
10	2.9000	1.615	0.176494	2.8000	1.080	0.170384	2.9000	3.610	0.096700
11	2.9091	1.785	0.186608	2.8182	1.200	0.166756	2.9091	3.990	0.100898
12	2.9167	1.955	0.190074	2.8333	1.320	0.196678	2.9167	4.370	0.104198
13	2.9231	2.125	0.194894	2.8462	1.440	0.194806	2.9231	4.750	0.106290
14	2.9286	2.295	0.199140	2.8571	1.560	0.198964	2.9286	5.130	0.107800
15	2.9333	2.465	0.203000	2.8667	1.680	0.200590	2.9333	5.510	0.108776
16	2.9375	2.635	0.206530	2.8750	1.800	0.207008	2.8375	5.890	0.109378
17	2.9412	2.805	0.209696	2.8824	1.920	0.210670	2.9412	6.270	0.109756
18	2.9444	2.975	0.212574	2.8889	2.040	0.212736			
19	2.9474	3.145	0.215078	2.8947	2.160	0.216286			
20	2.9500	3.315	0.217286	2.9000	2.280	0.219574			
21	2.9524	3.485	0.219250	2.9048	2.400	0.222596			
22	2.9545	3.655	0.220878	2.9091	2.520	0.225152			
23	2.9565	3.825	0.222274	2.9130	2.640	0.227982			
24	2.9583	3.995	0.223498	2.9167	2.760	0.230534			
25	2.9600	4.165	0.224426	2.9200	2.880	0.233308			
26	2.9615	4.335	0.224722	2.9231	3.000	0.235456			
27	2.9630	4.505	0.225854	2.9259	3.120	0.237614			
28	2.9643	4.675	0.226266	2.9286	3.240	0.239736			
29	2.9655	4.845	0.226582	2.9310	3.360	0.241932			
30	2.9667	5.015	0.226858	2.9333	3.480	0.243640			
31	2.9677	5.185	0.226916	2.9355	3.600	0.245388			
32	2.9688	5.355	0.226942	2.9375	3.720	0.247030			
33	2.9697	5.525	0.226978	2.9394	3.840	0.248782			
34	2.9706	5.695	0.226824	2.9412	3.960	0.250048			
35				2.9429	4.080	0.251386			
36				2.9444	4.200	0.252582			
37				2.9459	4.320	0.253984			
38				2.9474	4.440	0.254838			
39				2.9487	4.560	0.255822			
40				2.9500	4.680	0.256684			
41				2.9512	4.800	0.257784			
42				2.9524	4.920	0.258304			
43				2.9535	5.040	0.259008			
44				2.9545	5.160	0.259604			
45				2.9556	5.280	0.260460			
46				2.9565	5.400	0.260726			

The values of d_x refer to idealized structures and are calculated using the formulae below, using $a = 0.38$ nm. The value of x and n are those pertaining to an ordered array of c.s. planes of separation d_x.

{102} c.s. planes, W_nO_{3n-1}, $x = (3n-1)/n$, $d_x = (n-\frac{1}{2})a/\sqrt{5}$

{103} c.s. planes, W_nO_{3n-2}, $x = (3n-2)/n$, $d_x = (n-1)a/\sqrt{10}$

{001} c.s. planes, W_nO_{3n-1}, $x = (3n-1)/n$, $d_x = (n-\frac{1}{2})a$.

PHILOSOPHICAL TRANSACTIONS OF THE ROYAL SOCIETY A MATHEMATICAL, PHYSICAL & ENGINEERING SCIENCES

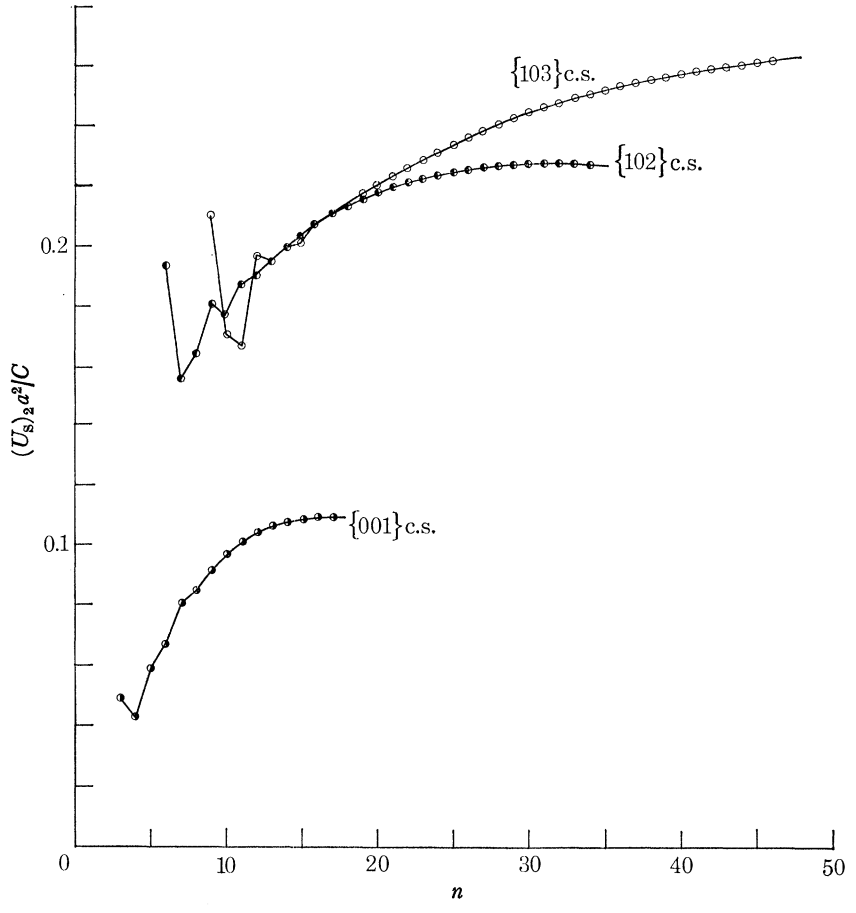

FIGURE 8. The elastic strain energy between a pair of {102}, {103} or {001} c.s. planes, $(U_s)_2 a^2/C$ plotted as a function of the number of octahedra, n, between them.

6. DISCUSSION

The results obtained in these calculations can be conveniently discussed in two parts, firstly a consideration of the forms and relative magnitudes of the $(U_s)_1$ and $(U_s)_2$ curves themselves and secondly a discussion of the elastic strain energy of crystals containing c.s. planes. We will take these in turn, in the sections below.

(a) *The $(U_s)_1$ and $(U_s)_2$ curves*

One of the most noticeable features of the strain energy calculations is that the values of $(U_s)_1$ and $(U_s)_2$ for {001} c.s. planes are rather small compared to both the {102} and {103} cases. This would seem to be quite reasonable in the light of the physical structure of the c.s. planes. In both the {102} and {103} c.s. planes we find discontinuities consisting of pairs of 'empty octahedra' between the units of edge-shared octahedra which make up the c.s. planes. These discontinuities were found to have a considerable effect on the strain field in the neighbourhood of the c.s. plane, the calculations showing that the strain energies of the W ions located nearest to isolated {102} and {103} c.s. planes were considerably higher than their {001} counterparts. A major part of the total elastic strain due to a c.s. plane is therefore due to the discontinuous nature of the {102} and

{103} c.s. planes. Physically it is possible that these 'empty octahedra' will allow a considerable relaxation of the internal strain energy of these c.s. planes, U_{self}, to occur. If this is so one would expect that {001} c.s. planes would have proportionately higher values of U_{self} than {102} and {103} c.s. planes. This will be of some importance when the formation energy of c.s. planes is considered and perhaps make {001} c.s. planes somewhat more difficult to form than simple bond energy considerations would suggest (Tilley 1976). It should also be borne in mind in the following sections, where relative values of U_{self} for these c.s. plane types are discussed in more detail.

As the discontinuities in the c.s. plane are in a large measure responsible for the higher strain energy of the {102} and {103} c.s. planes compared to the {001} geometry one would expect that both the $(U_s)_1$ and $(U_s)_2$ curves for the series {102}, {103} ... {10m} ... {001} would pass through a maximum, probably near to {104} or {105} and then fall to the final value of {001}. As the amount of computation needed to verify this is considerable and is not yet complete, the results will be presented in the future. Such a situation, though, would have an appreciable effect upon the microstructures of crystals containing c.s. planes, with indices higher than {103}. A further discussion of this will be given when the results of these additional calculations are completed.

In an analogous way to the fashion in which the elastic strain energy of a {10m} c.s. plane should approach that of an {001} c.s. plane as m tends to higher values, so one would expect the value of $(U_s)_2$ to approach $2(U_s)_1$ as the separation between the c.s. plane pair increases. An examination of the results shows that the $(U_s)_2$ curves should thus also pass through a maximum value. In the case of {102} c.s. planes the computations have been carried far enough to locate this position, which corresponds to an n value of 33 and a c.s. plane spacing of approximately 5.525 nm. The computations have not been carried so far in the cases of the {103} and {001} c.s. planes but it seems reasonable to suppose that they will behave in a similar fashion and that maxima will also occur in their $(U_s)_2$ curves also. In such a situation, when the composition of a reduced crystal lies between WO_3 and the maximum on any of the $(U_s)_2$ curves, the elastic strain energy will fall as the c.s. plane separation *increases*. On the other hand, when the composition is lower than the maximum, the elastic strain energy will fall as the c.s. plane separation *decreases*. Physically, these differences may be considered to give rise to a virtual repulsive force between c.s. planes at high separations and to a virtual attractive force between c.s. planes at low separations. It is not certain, however, whether the energy changes involved would be sufficient to cause the c.s. planes to move in a crystal, as the ionic mobility necessary is dependent upon a large number of factors, especially temperature.

The existence of quite distinct peaks and valleys in the $(U_s)_2$ curves is of some interest. In general it is apparent from figure 8 that the values for $(U_s)_2$ lie on smooth curves until the lower n values are reached. At this point it appears that some particular c.s. plane separations have a higher elastic strain between them than their near neighbours. In the {102} case these higher strain values are at $n = 6$, 9 and 11, in the {103} case at 9, 10, 12, 13, 14, 16 and 17, and in the {001} case at n values of 3, 5 and 7. This feature of the curves suggests that pairs of c.s. planes with spacings equal to these higher strain values will not form, as a slight movement of the c.s. planes will allow the strain energy to fall measurably. The more important significance of these features, though, pertains to their influence upon the microstructure of the bulk crystals, and as such will be considered in more detail below.

PHILOSOPHICAL TRANSACTIONS OF THE ROYAL SOCIETY A MATHEMATICAL, PHYSICAL & ENGINEERING SCIENCES

(b) The elastic strain energy of crystals containing ordered arrays of c.s. planes

We will consider here the case where a substantial degree of reduction has taken place so that a crystal can be considered to contain an ordered array of either {102}, {103} or {001} c.s. planes and to be a member of either the W_nO_{3n-1} or W_nO_{3n-2} homologous series of oxides. Referring to figure 6, if a crystal has a composition x, then the increase in elastic strain energy per unit volume of the crystal will be given by (U_x/L). The number of c.s. planes introduced into the crystal, N_x is related to the spacing between the c.s. planes d_x by the equation

$$N_x d_x = L.$$

(U_x/L) can then be written as

$$\begin{aligned}(U_x/L) &= (N_x U_{self})/L + (N_x - 1)\,(U_s)_2/L + (U_s)_1/L \\ &= U_{self}/d_x + (N_x - 1)\,(U_s)_2/N_x d_x + (U_s)_1/N_x d_x,\end{aligned}$$

and as we are supposing N_x is high, i.e. $N_x \gg 1$

$$(U_x/L) \simeq [U_{self} + (U_s)_2]/d_x. \tag{20}$$

Therefore, for a {102}, {103} or {001} c.s. plane array we can write

$$(U_x/L)_{102} \simeq [U_{self} + (U_s)_2]_{102}/(d_x)_{102}, \tag{20a}$$

$$(U_x/L)_{103} \simeq [U_{self} + (U_s)_2]_{103}/(d_x)_{103}, \tag{20b}$$

$$(U_x/L)_{001} \simeq [U_{self} + (U_s)_2]_{001}/(d_x)_{001}. \tag{20c}$$

The approximate spacing between the c.s. planes, d_x, can be readily calculated and values are tabulated in table 2. It is seen that for any composition WO_x the spacing of {103} c.s. planes is $\sqrt{2}$ that of {102} c.s. planes. That is, $\sqrt{2}$ times as many {102} c.s. planes need to be introduced to reach the composition of WO_x as {103} c.s. planes. Similarly, for {001} the spacing is $\sqrt{5}$ times that for {102} c.s. planes.

From the data in table 2, plots of $(U_s)_2/(d_x)$ against composition, x, for {102} and {103} c.s. have been constructed and are shown in figure 9. These reveal that the strain energy density in the crystal increases as the number of c.s. planes in the crystal increases. As figure 9 and table 2 show, we can write

$$[(U_s)_2]_{001}/(d_x)_{001} < [(U_s)_2]_{103}/(d_x)_{103} < [(U_s)_2]_{102}/(d_x)_{102}. \tag{21}$$

However, in order to discuss the real magnitude of U_x/L we need to make some reasonable assumptions about the magnitude of U_{self}. For this, we have suggested,

$$(U_{self})_{102} = 2U_0/3, \quad (U_{self})_{103} = 3U_0/4, \tag{22a}$$

where U_0 is a constant which is the value of U_{self} for a continuous c.s. plane lying along {001} and shown in figure 1, i.e.

$$(U_{self})_{001} = U_0. \tag{22b}$$

This assumption is simply based upon the supposition that an edge sharing octahedron in a c.s. plane has a uniquely determined energy U_{self} which is independent of the c.s. plane structure, although, as mentioned in section 6 (*a*), U_0 for an {001} c.s. plane may be higher than this simple approach suggests. The factors $\frac{2}{3}$ and $\frac{3}{4}$ follow simply from the geometry of the {102}, {103} and

PHILOSOPHICAL TRANSACTIONS OF THE ROYAL SOCIETY A MATHEMATICAL, PHYSICAL & ENGINEERING SCIENCES

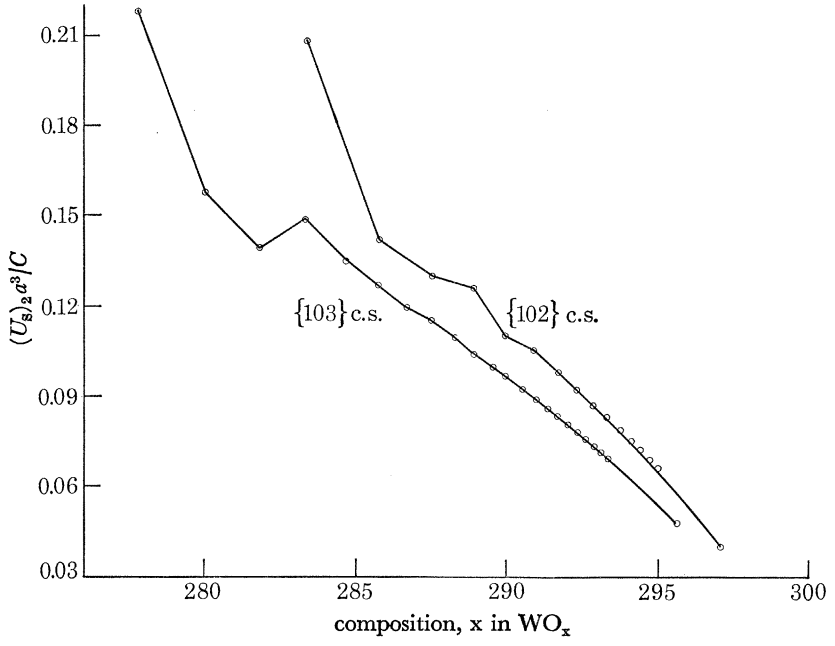

FIGURE 9. The elastic strain energy per unit volume $(U_s)_2/d_x$ for an ordered array of {102} or {103} c.s. planes plotted as a function of the composition of the crystal x in WO_x. The theoretical points have been omitted from the part of the curve at higher x values for clarity.

{001} c.s. planes, as a {102} c.s. plane has 4 edge sharing octahedra and two 'empty' octahedra in a unit, the {103} c.s. plane has 6 edge sharing octahedra and 2 'empty' octahedra in a unit while the {001} c.s. plane has no 'empty' octahedra present.

Thus, if we write $S = (d_x)_{102}$ then at any composition x,

$$(U_{self})_{102}/(d_x)_{102} = (2U_0/3)/S = 0.667\,(U_0/S),$$

$$(U_{self})_{103}/(d_x)_{103} = (3U_0/4)/\sqrt{2}\,S = 0.530\,(U_0/S),$$

$$(U_{self})_{001}/(d_x)_{001} = U_0/\sqrt{5}\,S = 0.477\,(U_0/S),$$

i.e.
$$(U_{self})_{001}/(d_x)_{001} < (U_{self})_{103}/(d_x)_{103} < (U_{self})_{102}/(d_x)_{102}. \qquad (23)$$

As we assume that the values of U_{self} do not vary with composition the general shape of each curve in figure 9 will be unchanged, but now they will rise more steeply as the composition falls. The addition of this U_{self} term will not cause the curves to cross over at all so that we can assume that at any particular composition x a crystal containing {001} c.s. planes will have the lowest elastic strain energy and a crystal containing {102} c.s. planes the highest.

This result indicates that the elastic strain energy is not directly responsible for the sequence of c.s. plane families observed when WO_3 is reduced, for in this case {102} c.s. planes form initially, then {103}, {104} and ultimately {001}. If the formation criterion was solely to minimize strain energy, {001} would be expected both to form initially and also to be the preferred type in ordered arrays. The formation energy of c.s. planes must therefore involve alternative energy terms, of which the energy required to remove oxygen atoms from the WO_3 lattice would seem to be of prime importance (Tilley 1976).

The elastic strain energy would, however, be expected to influence the microstructures of crystals containing ordered arrays of c.s. planes to some extent. Experimental evidence to test

this is unfortunately sparse. The mixed $(Mo, W)_nO_{3n-1}$ oxides containing ordered {102} c.s. planes have been studied in some detail some years ago (Magnéli, Blomberg-Hansson, Kihlborg & Sundkvist 1955). These authors were mainly investigating the oxides between $(Mo, W)_{10}O_{29}$ and $(Mo, W)_{14}O_{41}$, and concluded that the oxides with n odd, namely, $(Mo, W)_9O_{26}$, $(Mo, W)_{11}O_{32}$ and $(Mo, W)_{13}O_{38}$ were not readily formed and were unstable compared to oxides with n even. An examination of figure 9 shows that the oxides M_7O_{20}, M_9O_{26} and $M_{11}O_{32}$ do have a greater strain energy per unit volume than their neighbours with n even, which suggests that they will be less stable than their neighbours. The situation can be analysed in more detail using the results already obtained.

Suppose that a sample of composition $(M, W)O_{3-x}$ is prepared in a sealed ampoule and that the composition corresponds exactly to an oxide of formula M_nO_{3n-1}. In some circumstances the oxide will have a strain energy lower than its immediate neighbours, $M_{n+1}O_{3(n+1)-1}$ and $M_{n-1}O_{3(n-1)-1}$ while in other cases disproportionation into these neighbours will result in an overall lowering of the elastic strain energy in the sample. It is reasonable to suppose that in this latter case the tube will contain more of the oxides $M_{n+1}O_{3(n+1)-1}$ and $M_{n-1}O_{3(n-1)-1}$ than the oxide M_nO_{3n-1} and one would conclude that the $(n+1)$ and $(n-1)$ oxides were more stable. The situation of lowest strain energy would ultimately be reached when none of the M_nO_{3n-1} oxide remained.

Imagine a crystal of the oxide M_nO_{3n-1} to contain N c.s. planes. The elastic strain energy due to these c.s. planes will be

$$\begin{aligned}(U_s)^n &= N U_{self} + (U_s)_1 + (N-1)\,(U_s)_2^n \\ &\simeq N U_{self} + N\,(U_s)_2^n. \end{aligned} \tag{24}$$

Simply by redistributing the N c.s. planes laterally, without changing their total number, we can formally convert the original crystal into a bicrystal containing the two oxides $M_nO_{3(n+1)-1}$ and $M_nO_{3(n-1)-1}$. In this process the total number of c.s. planes and the total surface area of the crystal does not change. The number of c.s. planes associated with each of the two oxides is $\frac{1}{2}N$. The elastic strain energy of the crystal is now $(U_s)^{n'}$, where

$$\begin{aligned}(U_s)^{n'} &= N U_{self} + (U_s)_1 + (\tfrac{1}{2}N-1)\,(U_s)^{n-1} + (\tfrac{1}{2}N)\,(U_s)_2^{n+1} \\ &\simeq N U_{self} + \tfrac{1}{2}N(U_s)^{n-1} + \tfrac{1}{2}N\,(U_s)_2^{n+1} \\ &\simeq N U_{self} + \tfrac{1}{2}N[(U_s)_2^{n-1} + (U_s)_2^{n+1}]. \end{aligned} \tag{25}$$

Some further consideration reveals that this analysis is also true if the sample consists of many crystals which disproportionate, instead of just a single crystal. Hence, in a normal sample, the disproportionation can be made without a change in the total surface area, number of c.s. planes or number of crystals. The net change in elastic strain energy is then given by $[(U_s)^n - (U_s)^{n'}]$, i.e.

$$\Delta(U_s)^n_{n'} = (U_s)^n - (U_s)^{n'} = N[(U_s)_2^n - \tfrac{1}{2}\,(U_s)_2^{n+1} - \tfrac{1}{2}\,(U_s)_2^{n-1}]. \tag{26}$$

We can therefore say that if $\Delta(U_s)^n_{n'}$ is positive, the oxide M_nO_{3n-1} has a higher overall elastic strain energy, and the sample would gain by a disproportionation. If, on the other hand $\Delta(U_s)^n_{n'}$ is negative, disproportionation would increase the strain energy in the system. The values of $\Delta(U_s)^n_{n'}$ for {102} c.s. planes are listed in table 3.

An examination of the values shown in table 3 reveal that, from the point of view of elastic strain energy, only the oxides M_7O_{20}, M_8O_{23}, $M_{10}O_{29}$ and $M_{12}O_{35}$ are stable. This agrees well with the more qualitative observations of Magnéli *et al.* mentioned above, as in the composition

PHILOSOPHICAL TRANSACTIONS OF THE ROYAL SOCIETY A MATHEMATICAL, PHYSICAL & ENGINEERING SCIENCES

TABLE 3. STABILITY OF HOMOLOGOUS OXIDES BASED UPON MINIMUM ELASTIC STRAIN ENERGY

	{102} c.s.			{103} c.s.			{001} c.s.		
n	$\frac{1}{2}[(U_S)_2^{n-1}+(U_S)_2^{n+1}]a^2/C$	$\Delta(U_S)_n^n a^2/C$	stability†	$\frac{1}{2}[(U_S)_2^{n-1}+(U_S)_2^{n+1}]a^2/C$	$\Delta(U_S)_n^n a^2/C$	stability†	$\frac{1}{2}[(U_S)_2^{n-1}+(U_S)_2^{n+1}]a^2/C$	$\Delta(U_S)_n^n a^2/C$	stability†
3							—	—	—
4							0.053987	−0.011441	S
5							0.054670	+0.004396	U
6	—	—	—				0.069676	−0.002882	S
7	0.179383	−0.023617	S				0.075669	+0.004617	U
8	0.168511	−0.003773	S				0.085794	−0.001250	S
9	0.170616	+0.010640	U	—	—	—	0.090622	+0.000680	U
10	0.183932	−0.007438	S	0.188379	−0.017995	S	0.096100	+0.000600	U
11	0.183284	+0.003324	U	0.183531	−0.016775	S	0.100449	+0.000449	U
12	0.190751	−0.000677	S	0.180781	+0.015897	U	0.103594	+0.000604	U
13	0.194607	+0.000287	U	0.197821	−0.003015	S	0.105999	+0.000291	U
14	0.198947	+0.000193	U	0.197698	+0.001266	U	0.107533	+0.000267	U
15	0.202835	+0.000165	U	0.202986	−0.002396	S	0.108589	+0.000187	U
16	0.206348	+0.000182	U	0.205630	+0.001378	U	0.109266	+0.000112	U
17	0.209552	+0.000144	U	0.209872	+0.000798	U			
18	0.212387	+0.000187	U	0.213478	−0.000742	S			
19	0.214930	+0.000148	U	0.216155	+0.000131	U			
20	0.217164	+0.000122	U	0.219441	+0.000133	U			
21	0.219082	+0.000168	U	0.222363	+0.000235	U			
22	0.220762	+0.000116	U	0.225289	−0.000137	S			
23	0.222188	+0.000086	U	0.227843	+0.000139	U			
24	0.223350	+0.000148	U	0.230645	−0.000111	S			
25	0.224110	+0.000316	U	0.232995	+0.000313	U			
26	0.225140	−0.000418	S	0.235461	−0.000005	S			
27	0.225494	+0.000360	U	0.237596	+0.000018	U			
28	0.226218	+0.000048	U	0.239773	−0.000037	S			
29	0.226562	+0.000020	U	0.241688	+0.000244	U			
30	0.226749	+0.000109	U	0.243660	−0.000020	S			
31	0.226900	+0.000016	U	0.245335	+0.000053	U			
32	0.226947	−0.000005	S	0.247085	−0.000055	S			
33	0.226883	+0.000095	U	0.248539	+0.000243	U			
34				0.250084	−0.000036	S			
35				0.251315	+0.000071	U			
36				0.252685	−0.000103	S			
37				0.253710	+0.000274	U			
38				0.254903	−0.000065	S			
39				0.255761	+0.000061	U			
40				0.256803	−0.000119	S			
41				0.257494	+0.000290	U			
42				0.258396	−0.000092	S			
43				0.258954	+0.000054	U			
44				0.259734	−0.000130	S			
45				0.260165	+0.000295	U			

† S, Stable; U, unstable.

range that they studied oxides $(Mo, W)_n O_{3n-1}$ with n odd are indeed less stable than their even n value neighbours. A further conclusion can also be drawn from the calculations. If we consider a sample of composition $(Mo, W)O_{2.95}$ corresponding to an oxide $(Mo, W)_{20}O_{59}$, it is found that the elastic strain energy will be less if a mixture of oxides $(Mo, W)_{19}O_{57}$ and $(Mo, W)_{21}O_{62}$ forms rather than a single phase of formula $(Mo, W)_{20}O_{59}$. However, both $(Mo, W)_{19}O_{57}$ and $(Mo, W)_{21}O_{62}$ are unstable with respect to further disproportionation. A continuation of the

disproportionation process ultimately results in $(Mo, W)_{12}O_{35}$ and an oxide close to WO_3 which, experimentally, will consist of slightly reduced WO_{3-x} containing isolated {102} c.s planes or clusters of such {102} c.s. planes. Of course the reaction path is unlikely to involve this hypothetical disproportionation route, but a more direct reaction to $(Mo, W)_{12}O_{35}$ $(MO_{2.92})$ and slightly reduced WO_3. This too is in good agreement with the findings of Magnéli *et al.*, for in samples of gross composition above about $MO_{2.92}$ they found a 'two phase' mixture of M_nO_{3n-1} oxides and WO_3. More recent electron microscope studies of reduced tungsten oxides also reveals no tendency for reduction of WO_3 to result in stable homologues of the W_nO_{3n-1} series with compositions in the range of $WO_{2.93}$ to $WO_{2.97}$ unless large crystals are employed in which case a nucleation mechanism like that discussed in the following section can be invoked (Sundberg & Tilley 1974; Iguchi & Tilley, to be published).

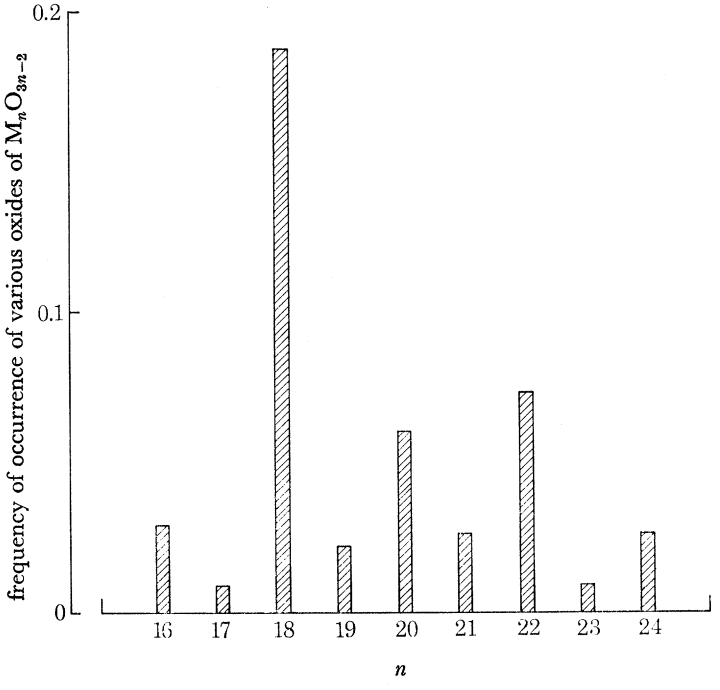

FIGURE 10. Histrogram showing the frequency of occurrence of various tungsten oxides of the homologous series M_nO_{3n-2} prepared in sealed ampoules and heated 2 weeks × 1100 °C.

The case of {103} c.s. planes can be treated in an identical way. The equations (24)–(26) do not change, and table 3 shows $\Delta(U_s)^n_{n'}$ values relevant to the {103} case. From this table it is apparent that for most n values every other n value is preferred although for the lower n values the distribution becomes irregular. There is no information available in the previous literature with which to compare the theoretical results, except for the observation by Bursill & Hyde (1972) that every third n value of the series W_nO_{3n-2} would be expected to be preferred. Because of this we undertook a statistical survey of $(M, W)_nO_{3n-1}$ and $(M, W)_nO_{3n-2}$ oxides that were present in sealed tube preparations with overall compositions between $(M, W)O_{2.80}$ and $(M, W)O_{2.97}$. The bulk of these results will be published later, but in figure 10 we have shown a histogram summarizing the occurrence of {103} c.s. phases in samples prepared in the ternary Ge–W–O system and which may contain a trace of germanium. No oxides were found with n values greater than 24 or less than 16. This latter figure is in good agreement with published data on the binary tungsten

oxides, where $W_{16}O_{47}$ was also the lowest oxide found before the tunnel phase $W_{18}O_{49}$ formed (Pickering & Tilley 1976). In general it is seen that the agreement between figure 10 and table 3 is good as the oxides encountered most frequently are also those expected to be preferred in terms of lowest elastic strain energy.

A comparison of the $\Delta(U_s)^n_{n'}$ results for {102} c.s. and {103} c.s. phases reveals a significant difference in behaviour. In the case of {102} c.s. phases it was shown that a sample of composition higher than approximately $MO_{2.92}$ would disproportionate into slightly reduced WO_3 and $M_{12}O_{35}$ as far as stoichiometry would allow. In the case of {103} c.s. planes no such extensive disproportionation need take place, and compositions in this middle range can always be accommodated by the formation of one or two stable M_nO_{3n-2} oxides which are not far removed from the gross stoichiometry of the preparation. Again this finding is in good agreement with previous studies on {103} c.s. phases (Allpress & Gadó 1970; Bursill & Hyde 1972).

The microstructure to be found in crystals containing {001} c.s. planes are not known in any detail at all, although it is certain that fairly well ordered $(M, W)_n O_{3n-1}$ oxides do form in the Nb–W–O and Ti–W–O ternary systems (Allpress 1972; Bursill & Hyde 1972; Ekström & Tilley 1974). In this case we have also calculated the values of $\Delta(U_s)^n_{n'}$ and listed them in table 3 but in view of the lack of experimental data a comparison with observation has not been made.

It is apparent from table 3 that for higher n values in both the {102} c.s., {103} c.s. and {001} c.s. only slight changes in the $(U_s)_2$ values will alter the sign of $\Delta(U_s)^n_{n'}$ and so alter the relative stabilities of various members of the two homologous series of oxides. In view of the approximations made in evaluating $(U_s)_2$ the agreement between experiment and calculation is rather better than would be expected and does add further to the conclusion that elastic strain energy does indeed play an important role in influencing the micro-structures of these crystals.

(c) *Nucleation and growth* {102} *c.s. planes*

Although the elastic strain energy of isolated {001} c.s. planes is much lower than that of isolated {102} or {103} c.s. planes, initial reduction of WO_3 crystals always leads to the formation of isolated {102} c.s. planes indicating that the formation energy of {102} c.s. planes must be considerably lower than that of the other two c.s. plane types, and must dominate the elastic strain energy terms. Somewhat further reduction not only increases the number of isolated c.s. planes in the crystal, but also causes pairs and small clusters of c.s. planes to form. This type of microstructure may well be sensitive to the elastic strain fields of the c.s. planes and can be analysed using the results presented in figures 7 and 8.

If we suppose that an initial reaction produces a {102} c.s. plane in WO_3 we can now consider the possibility that a second c.s. plane forms either in a remote position, or close by to form a pair. The strain energy of a pair of c.s. planes $(U)_{\text{pair}}$ will be

$$\begin{aligned}(U)_{\text{pair}} &= 2U_{\text{self}} + (U_s)_1 + (U)_2 \\ &= 2(U)_{\text{isol.}} + [(U_s)_2 - (U_s)_1],\end{aligned} \tag{27}$$

where $(U)_{\text{isol.}}$ is the strain energy associated with an isolated c.s. plane given by $(U)_{\text{isol.}} = U_{\text{self}} + (U_s)_1$. In this case, when $[(U_s)_2 - (U_s)_1]$ is negative, i.e. $(U_s)_2 < (U_s)_1$, the value of $(U)_{\text{pair}}$ will be less than $2(U)_{\text{isol.}}$ and pair formation will be favoured.

In figure 11, we have plotted $[(U_s)_2 - (U_s)_1]$ as a function of n. The vertical axis of this figure shows $[(U_s)_2 - (U_s)_1]\, a^2/C$. According to this result, less energy will be expended if two {102}

c.s. planes form a pair with a separation between them of less than $n = 20$ corresponding to an oxide $W_{20}O_{58}$ with a c.s. plane spacing of about 2.95 nm. Experimentally, nucleation of new {102} c.s. planes near to existing ones has been observed both by Iijima (1975) and in this laboratory. Figure 12 shows a typical instance.

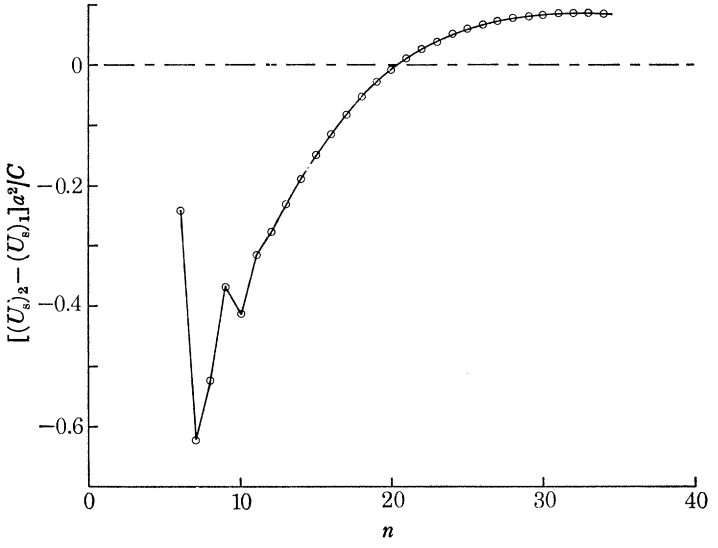

FIGURE 11. The difference between the energy of a pair of {102} c.s. planes and two isolated c.s. planes, $[(U_s)_2-(U_s)_1]$, plotted as a function of the separation between them, n. Pairs will form for negative values of $[(U_s)_2-(U_s)_1]$.

From figure 12*a*, plate 1, we can estimate the separation between the original pair of c.s. planes to correspond to $n = 39$ in the formula W_nO_{3n-1}. The new c.s. planes, which are just forming in figure 12*b* can be seen clearly in figure 12*c*, from which we can estimate that they form at a separation of about 1.6 nm from the parent c.s. planes, corresponding to $n = 10$ in the formula W_nO_{3n-1}. The separation between the new c.s. planes corresponds to a formula $W_{19}O_{56}$, i.e. 3.15 nm. The idealized structure of this array is shown in figure 12*d*.

If we merely consider the strain energy values given it is necessary to conclude that the c.s. planes should nucleate at a position rather closer than 1.6 nm, as the valley corresponding to $n = 7, 8$ is the most favourable one energetically. The fact that this does not take place indicates the limitations of treating the $(U_s)_2$ terms in isolation. Clearly the elastic strain energy per unit volume will increase in the neighbourhood of the c.s. plane as can be seen from figure 9 and at some value this will become prohibitive. In addition, other interaction forces may start to dominate. These factors are unknown at present, but it would appear that they are effective when n (102) starts to fall below about 14.

We can also compare this result with the theory of Bursill & Hyde (1971) who suggested that the free energy of an array of c.s. planes in rutile should be a minimum when the spacing between the c.s. planes was equal. In the case shown in figure 12, this would be equivalent to $n = 13$. From table 2 we can see that the free energy per unit cross sectional area for this spacing is given by

$$0.584682C/a^2.$$

On the other hand, the free energy of the arrangement shown in figure 12*d* is

$$0.568066C/a^2,$$

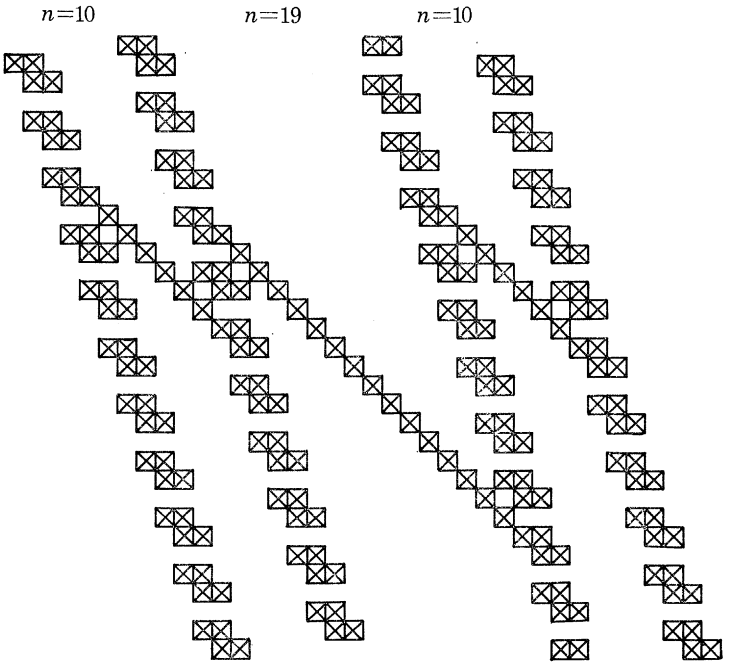

FIGURE 12(*d*). For legend see plate 1.

which is considerably lower than in the former case. This indicates that the more simple interaction curve suggested by these authors is not, in fact, in such good agreement with observations in the WO_{3-x} system.

Clearly we can consider nucleation of c.s. planes to continue, resulting in an increased c.s. plane density in the crystal. The new c.s. planes can either form close to existing c.s. planes in the manner just discussed, to ultimately form a cluster of c.s. planes, or, on the other hand, they can nucleate at random in the crystal. The analysis of the elastic strain energy involved in these two alternatives follows closely on that just described. Thus, if we have $N\{102\}$ c.s. planes arranged in a cluster, the strain energy, $(U)_c$, will be given

$$\begin{aligned}(U)_c &= N U_{self} + (U_s)_1 + (N-1)(U_s)_2 \\ &= N U_{isol.} + (N-1)[(U_s)_2 - (U_s)_1]. \end{aligned} \tag{28}$$

As before, therefore, a cluster will be preferred if $(U_s)_2 < (U_s)_1$, which is the same condition as found for pair formation described above.

There is, however, another factor which will be of importance in the case of cluster formation, the total elastic strain energy within the cluster. Examination of figure 9 and a consideration of the previous section shows that the elastic strain energy of a crystal containing large numbers of c.s. planes is higher than that of a crystal containing no c.s. planes. In the same way, the elastic strain energy of the volume of crystal containing the cluster of c.s. planes will be much greater than that of the surrounding matrix. The strain energy per unit volume will therefore fall as the c.s. planes get further apart. However, once the separation of the c.s. planes is greater than $n \simeq 20$, i.e. the condition when $(U_s)_2 = (U_s)_1$ the strain energy of the cluster becomes greater than the strain energy of N isolated c.s. planes. Thus for cluster formation by the nucleation mechanism outlined above, the most favourable balance between total elastic strain energy and elastic

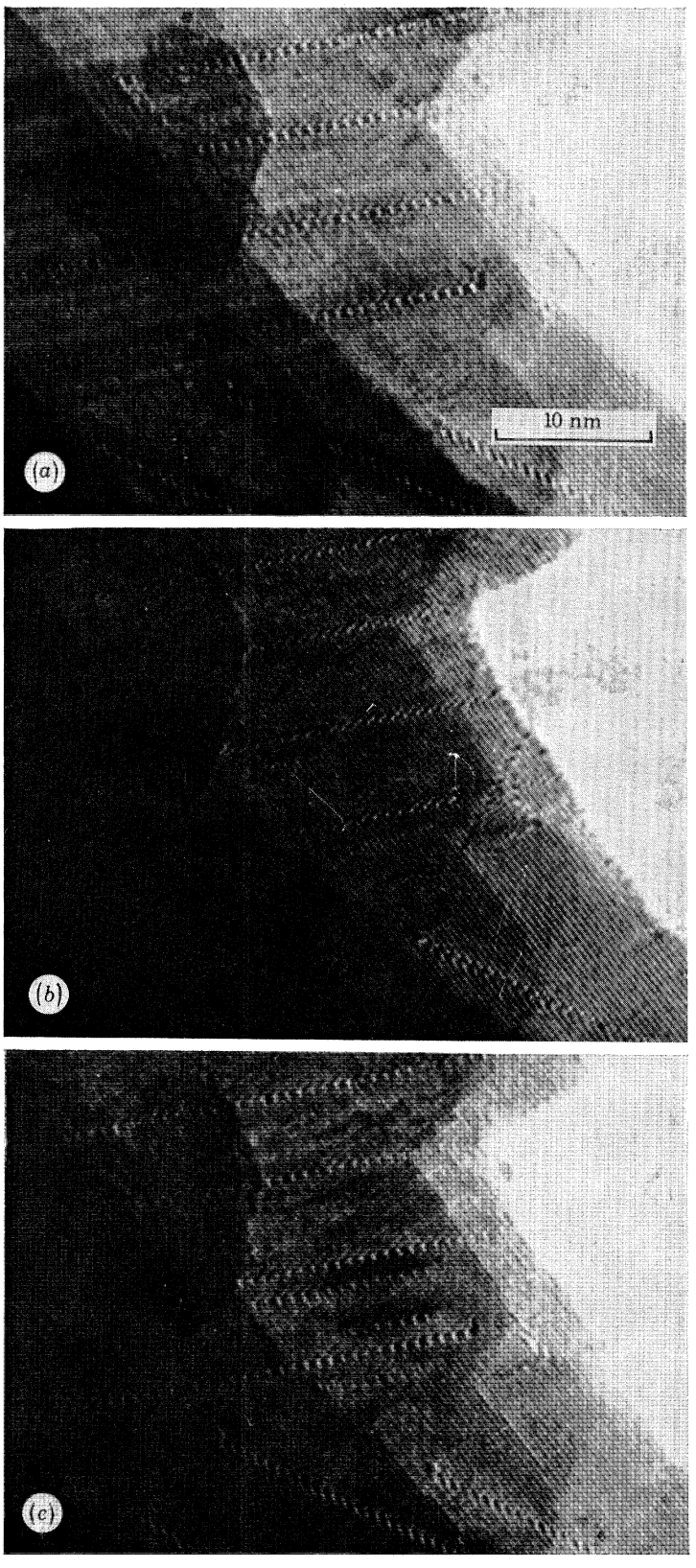

FIGURE 12. (*a–c*) Electron micrographs showing the growth of pairs of {102} c.s. planes near to isolated {102} c.s. planes in slightly reduced WO_3; (*d*) a diagrammatic representation of the c.s. plane pairs formed in (*a–c*).

(*Facing p.* 80)

PHILOSOPHICAL TRANSACTIONS OF THE ROYAL SOCIETY A MATHEMATICAL, PHYSICAL & ENGINEERING SCIENCES

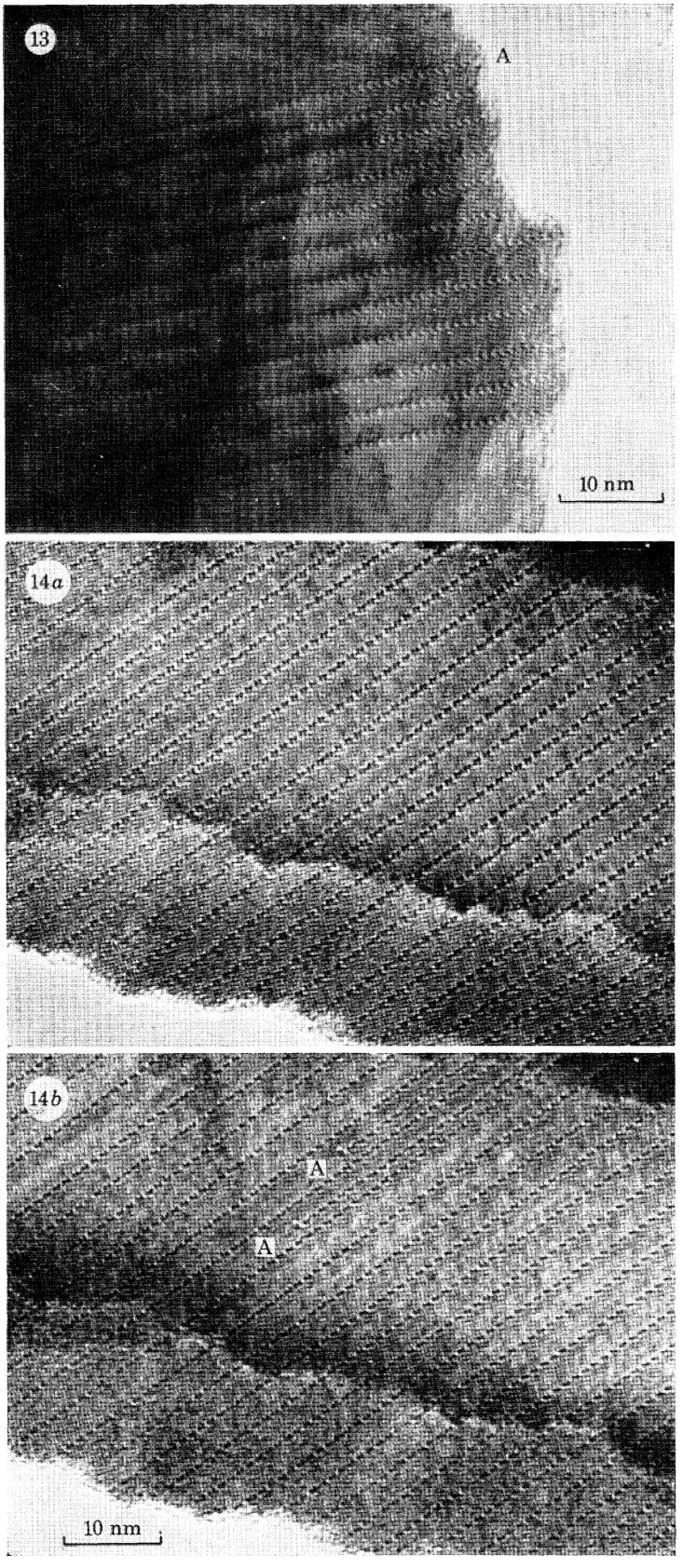

FIGURE 13. Electron micrograph of an isolated cluster of {102} c.s. planes in slightly reduced WO_3. The c.s. plane at A is in the process of growing into the crystal.

FIGURE 14 (*a*). Electron micrograph of a crystal containing quasi ordered {103} c.s. planes (*a*) before reduction in the electron microscope; (*b*) after observation, showing the growth of new c.s. planes, at A, A.

PHILOSOPHICAL TRANSACTIONS OF THE ROYAL SOCIETY A MATHEMATICAL, PHYSICAL & ENGINEERING SCIENCES

strain energy per unit volume is obtained when $[(U_s)_2 - (U_s)_1] = 0$, and one would expect a cluster to have c.s. plane spacings close to or slightly below that corresponding to $n = 20$.

An example of a cluster of {102} c.s. planes in slightly reduced WO_3 is shown in figure 13, plate 2. The estimated values of n, equivalent to the separation of the c.s. planes in the cluster, lie between 14 and 20 and the average value is 18. This is in good agreement with the present reasoning, and does suggest that the elastic strain energy is of some importance in determining the microstructure of such clusters. This figure also shows a new c.s. plane adding to the cluster at one end in further support of the general model of cluster formation outlined. It would therefore seem that clusters of c.s. planes, in slightly reduced WO_3 at least, are generated by a mechanism which involves preferential nucleation of c.s. planes near to existing ones at positions which result in a minimum increase in elastic strain energy. Inter-c.s. plane interactions will then serve to adjust the c.s. plane positions in the cluster to balance a variety of energy terms. The introduction of an alternative model for cluster formation in which randomly distributed c.s. planes come together under the influence of attractive interactions between c.s. planes does not seem necessary in these tungsten oxides, and, in the simplest case, inter-c.s. plane attractions are not at all necessary to produce a cluster of c.s. planes in the parent crystal matrix. It can also be noted that the cluster growth just described can continue to ultimately produce a large array of quasi-ordered {102} c.s. planes and so form a crystal of the W_nO_{3n-1} type.

Reference to figure 13 also reveals another feature of c.s. plane interactions in WO_3. There is no orderly variation of c.s. plane spacings as the group is traversed, and c.s. plane spacings at the edge of the cluster are no wider than those in the middle. Examination of other micrographs shows this to be the rule in slightly reduced WO_3 crystals. This behaviour seems to be quite different than that encountered in slightly reduced rutile, where the c.s. plane spacing at the edge of clusters is about twice that at the centre (Bursill & Hyde 1971). The form of the clusters in rutile was successfully analysed by Stoneham & Durham (1973) in terms of interactions between c.s. planes which extended over more than just nearest neighbours (see also §3). It would seem reasonable, in the case of clusters of {102} c.s. planes in WO_3, that such longer range interactions are not so important and their neglect, as in the present analysis, is not as serious as it would seem to be in the titanium oxides.

(*d*) *Nucleation and growth of* {103} *c.s. planes*

In crystals containing arrays of {103} c.s. planes, normal observation in the beam of an electron microscope often causes new c.s. planes to grow in between the existing set. They usually appear to come from the interior or thicker parts of the flake, grow parallel to their length and grow very rapidly, but can also be observed to nucleate in the thinner regions of the flake as well. They are not always exactly straight, and often wander a little from side to side, particularly if the original spacing is rather wide, say for example about 2.9 nm corresponding to an oxide $W_{26}O_{75}$. It is also found in such cases that the new c.s. plane lies to one side or the other of the centre of the original pair of c.s. planes and not in the middle. Figure 14, plate 2, shows a typical example of such c.s. plane growth. The results shown in figure 8 can explain this observation very well. According to our calculations, the increase in the elastic strain energy per unit area normal to the long axis (see figure 5) due to the nucleation of the new c.s. plane, U_n is given by equation (29).

$$U_n = U_{self} + [(U_s)_2]_{1n} + [(U_s)_2]_{n2} - [(U_s)_2]_{12}, \tag{29}$$

where U_{self} indicates the internal elastic strain of the new c.s. plane, $[(U_s)_2]_{1n}$ and $[(U_s)]_{n2}$ indicate

PHILOSOPHICAL TRANSACTIONS OF THE ROYAL SOCIETY A MATHEMATICAL, PHYSICAL & ENGINEERING SCIENCES

TABLE 4. ELASTIC STRAIN ENERGY OF SETS OF GROUPS OF THREE {103} C.S. PLANES

n	n_{1n}	n_{n2}	$(U_s)\ a^2/C$
24	12	12	0.393356
	10	14	0.369348
	11	13	0.361562
26	13	13	0.389612
	10	16	0.377392
	11	15	0.367346
28	14	14	0.397928
	10	18	0.383120
	11	17	0.377426
	13	15	0.395396
30	15	15	0.401180
	10	20	0.389958
	11	19	0.383042

the strain energy between the c.s. plane *1* and the new c.s. plane and that between the new c.s. plane and c.s. plane *2* respectively, and $[(U_s)_2]_{12}$ indicates the strain energy between the parent c.s. planes *1* and *2* before the new c.s. plane is nucleated. The term $\{U_{self} - [(U_s)_2]_{12}\}$ is constant and the value of U_n depends on the term $\{[(U_s)_2]_{1n} + [(U_s)_2]_{n2}\}$. The values of $[(U_s)_2]_{1n}$ and $[(U_s)_2]_{n2}$ clearly depend upon the appropriate values, n_{1n} between the c.s. plane *1* and the new c.s. plane and n_{n2} between the new c.s. plane and c.s. plane *2*. These values can be obtained from figure 8. In table 4, the values of $\{[(U_s)_2]_{1n} + [(U_s)_2]_{n2}\}$ for some couples of n_{1n} and n_{n2} are shown when the n values between the parent {103} c.s. planes are 24, 26, 28 and 30. According to this table, the value of $\{[(U_s)_2]_{1n} + [(U_s)_2]_{n2}\}$ for the couple $n_{1n} = n_{n2}$, which would be expected to have a minimum U_n value if the inter-c.s. plane potential proposed by Bursill & Hyde (1971) for reduced rutile holds, is not in fact the lowest possible value. Instead, the table shows that the new c.s. plane in each case should be nucleated at a position near to one of the parent c.s. planes, corresponding to a value of $n = 11$. This result fits the condition shown in figure 14 well. This behaviour is due to the fact that as n decreases $(U_s)_2$ decreases irregularly, and the valley corresponding to $n = 11$ is deep enough to control the sum of the terms $[(U_2)_2]_{1n}$ and $[(U_s)_2]_{n2}$.

7. CONCLUSIONS

The first conclusion that can be drawn from the present study is that the overall sequence of c.s. plane families found on reduction of tungsten trioxide, initially {102} followed by {103} and then {001}, is not controlled by elastic strain energy, for if that were so, {001} c.s. planes would always be preferred. The formation energy of c.s. planes is therefore governed by other factors which in the case of ternary c.s. phases will very likely include terms due to cation–cation and cation–anion–cation bonding within the c.s. plane. Nevertheless, when only one c.s. plane family is considered the agreement between the experimental results and the microstructures expected on the basis of considerations of strain energy is good, suggesting that elastic strain energy is indeed an important factor in determining which of several possible microstructures will be adopted by an array of c.s. planes.

If this is so it leads to several additional conclusions concerning the microstructures to be found in these crystals. Firstly we can note that the structure of WO_3 is not cubic but is in fact monoclinic at room temperature and tetragonal at temperatures of the order of 1000–1200 K where

many reactions are carried out. We would expect, therefore, a degree of anisotropy in the formation of c.s. planes because the cubic {102}, {103} and {001} sets will become non-equivalent in the real structure. Iijima (1975) has in fact reported such a result for c.s. planes in slightly reduced WO_3. It would be of some interest to attempt to calculate the differing elastic strain energies for the real crystal to compare with Iijima's findings, but this must wait, however, until the elastic constants of WO_3 itself are known.

The distortions found in WO_3 which will certainly effect the elastic ansotropy of the crystal are also found in the W_nO_{3n-2} oxides whose structures have been accurately determined and will also probably be present in all binary and ternary c.s. planes. These distortions vary from one homologue to the other and may well have a considerable influence upon the stability of the various members of a homologous series. The real distortions could therefore enhance the stability of some structures to an extent that they are strongly favoured over the others. A similar idea has been put forward by Magnéli (1970) who suggested that stability could be related to the pattern of metal-atom puckering above and below the mirror plane of the c.s. structure. This puckering will naturally reflect the mode by which the crystal structure attempts to minimize such constraints as elastic strain and the two ideas are thus closely parallel. As temperature will also affect these distortions it is possible to envisage the situation where the most stable homologue of a series of oxides changes with temperature. Experimental results to check such a suggestion are not yet available for the tungsten oxides.

Finally we can conclude that although elastic strain is important in influencing microstructures in these oxides, other factors become important at small c.s. plane spacings, as n values of less than 10 are rarely found. One such factor, already discussed, will be the elastic strain per unit volume of crystal, which increases rapidly at low c.s. plane separations. It is also possible that at these small spacings the c.s. planes begin to interact with each other electrostatically and the assumption of electrical neutrality becomes less realistic. In ternary systems such an effect may be enhanced by the preferential segregation of the dopant ions within the component octahedra of the c.s. plane. These problems are to be the subject of a further publication.

The authors are indebted to the Science Research Council for an equipment grant and for financial support for one of us (E.I.) and to Professor J. S. Anderson, F.R.S., for penetrating discussions of the results presented in this paper.

E.I. is also indebted to Professor R. Wada (Yokohama National University) for his encouragement during this work.

Appendix A. Evaluation of the forces responsible for elastic strain using an ionic model

The idealized structures of the c.s. planes are shown in figure 1. Considering first the {103} case, the charge distribution on the cations in the units has been chosen as $(4 \times 6 + 2 \times 4)e$ where e is the unit of electronic charge. Thus we suppose there to be $4W^{+6}$ cations and $2W^{+4}$ cations present. These were chosen on chemical grounds as the oxides WO_3 and WO_2 are well known while a formal oxide W_2O_5 does not exist. However, we take these merely as an example for the present, and other ionic distributions could readily be used.

Accepting that the interaction force between two ions is of a central force type (Pauling 1960)

we can assume that the nearest cations in the perfect WO_3 crystal have a relatively small interaction because there is an anion between these two nearest cations. In contrast in the unit of the c.s. plane, the cations in the (010) mirror planes interact directly with each other. This indicates that there are strong repulsive forces between nearest cations in the unit. In addition a repulsive force between nearest anions in the planes above and below the mirror planes is also expected, but this repulsive force is considered to be less strong than that between nearest cations in the mirror plane ($z = z_0$) because in an ionic model the charge on the anions is considerably lower than on the cations.

According to Pauling (1960) and Torrens (1972), the interatomic potential $\phi(r)$ between ion i and j can be approximately expressed as the following,

$$\phi(r) = \pm q_i q_j e^2/r + A \exp(-Br),$$

where q_i and q_j denote the charges of ion i and j, and r is the separation of these ions. Then, the repulsive force, $-f$, between these two ions is given by

$$-f = \frac{\alpha\phi}{\alpha r} = \mp q_i q_j e^2/r^2 - AB \exp(-Br).$$

As described above, one unit in the {103} c.s. plane has $32e$ charge due to the 6 cations. When the total $32e$ charge is assumed to be distributed equally between 6 cations, the repulsive force between two nearest cations in the unit of the {103} c.s. plane, f_{103} can be written as

$$f_{103} = (32/6)^2 e^2/r^2 + AB \exp(-Br).$$

In a similar way we can estimate the interaction forces for {102} and {001} c.s. planes. In these cases the repulsive forces, f_{102} and f_{001} become

$$f_{102} = (22/4)^2 e^2/r^2 + AB \exp(-Br),$$
$$f_{001} = (5)^2 e^2/r^2 + AB \exp(-Br).$$

These forces in each unit of {103}, {102} and {001} c.s. planes have been shown in figure 4. The forces on the anions at $z = z_0 \pm \frac{1}{2}$ will be in the same directions as those on the cations, as the spatial array is the same in both cases. These forces can be added to yield resultants in the plane $z = z_0$ which can then be included in the cationic repulsion terms.

Appendix B. Elasticity theory applicable to an isotropic continuum

The treatment follows that of Hirth & Lothe (1968). When a point force f is applied in the kth direction at the origin (0, 0, 0) in the isotropic continuum, the hth component of the displacement at (x, y, z), $u_{hk}(\boldsymbol{r})$ caused by the force f is given by the Green function

$$u_{hk}(\boldsymbol{r}) = \frac{1}{8\pi\mu}\left(\delta_{hk}\nabla^2 \boldsymbol{r} - \frac{\lambda + \mu\alpha^2 \boldsymbol{r}}{\lambda + 2\mu\alpha x_h \alpha x_k}\right),$$

where $\boldsymbol{r} = x\boldsymbol{i} + y\boldsymbol{j} + z\boldsymbol{k}$ and $\boldsymbol{i}, \boldsymbol{j}, \boldsymbol{k}$ indicate the unit vectors in the x, y, z axis respectively.

As the ReO_3-type crystal has cubic symmetry, we have the following relations between λ (the Lamé constant), μ (the shear modulus) and the elastic constants C_{11}, C_{12}, C_{44}.

$$\mu = C_{44} = \tfrac{1}{2}(C_{11} - C_{12}),$$
$$\lambda = C_{12}.$$

PHILOSOPHICAL TRANSACTIONS OF THE ROYAL SOCIETY A MATHEMATICAL, PHYSICAL & ENGINEERING SCIENCES

In the case that point forces f_x and f_y ($|f_x| = |f_y| = f$) are applied in the direction of the x and y axes at the origin $(0, 0, 0)$ in the isotropic continuum, the x, y and z component of the displacement at (x, y, z), u_1, u_2 and u_3 are given by

$$u_1 = u_{11}(r) + u_{12}(r)$$

$$u_2 = u_{21}(r) + u_{22}(r)$$

$$u_3 = u_{31}(r) + u_{32}(r),$$

here, the subscripts, 1, 2 and 3, denote the x, y and z components of a physical value.

References

Ackermann, R. J. & Sorrell, C. A. 1970 *J. High Temp. Sci.* **2**, 119–130.
Allpress, J. G. 1972 *J. Solid State Chem.* **4**, 173–185.
Allpress, J. G. & Gadó, P. 1970 *Crystal Lattice Defects* **1**, 331–342.
Anderson, J. S. 1972 *Surface and defect properties of solids*, **1**, (eds J. M. Thomas & M. W. Roberts), pp. 1–53, London: The Chemical Society.
Anderson, J. S. & Tilley, R. J. D. 1974 *Surface and defect properties of solids*, **3**, (eds J. M. Thomas & M. M. Roberts), pp. 1–56. London: The Chemical Society.
Bursill, L. A. & Hyde, B. G. 1971 *Phil. Mag.* **23**, 3–15.
Bursill, L. A. & Hyde, B. G. 1972 *J. Solid State Chem.* **4**, 430–446.
Ekström, T. 1975 *Chem. Comm. Univ. Stockholm* No. **7**.
Ekström, T. & Tilley, R. J. D. 1974 *Mater. Res. Bull.* **9**, 705–713.
Ekström, T. & Tilley, R. J. D. 1976 *J. Solid State Chem.* **18**, 123–131.
Eyring, L. & O'Keefe, M. 1970 *The chemistry of extended defects in non-metallic solids*, pp. 661–667. Amsterdam: North-Holland.
Gadó, P. 1974 *Acta Tech. Acad. Sci. Hung.* **78**, 317–324.
Hirth, J. P. & Lothe, J. 1968 *Theory of dislocations*, p. 29. New York: McGraw-Hill.
Iijima, S. 1975 *J. Solid State Chem.* **14**, 52–65.
Loopstra, B. O. & Boldrini, P. 1966 *Acta Crystallogr.* **21**, 158–162.
Loopstra, B. O. & Rietveld, H. M. 1969 *Acta Crystallogr.* B**25**, 1420–1421.
Magnéli, A., Blomberg-Hansson, B., Kihlborg, L. & Sundkvist, G. 1955 *Acta. Chem. Scand.* **9**, 1382–1390.
Magnéli, A. 1970 In *The chemistry of extended defects in non-metallic solids*, (eds L. Eyring & M. O'Keeffe), pp. 148–163. Amsterdam: North-Holland.
Pauling, L. 1960 *The nature of the chemical bond.* Ithaca, N.Y., Cornell University Press.
Pickering, R. & Tilley, R. J. D. 1976 *J. Solid State Chem.* **16**, 247–255.
Roth, R. S. & Waring, J. L. 1966 *J. Res. Natl. Bur. Stds* **70**A, 281–303.
Salje, E. & Viswanathan, K. 1975 *Acta Crystallogr.* A**31** 356–359.
Shannon, R. D. & Prewitt, C. T. 1969 *Acta Crystallogr.* B**25** 925–946.
Stoneham, A. M. & Durham, P. J. 1973 *J. Phys. Chem. Solids* **34**, 2127–2135.
Sundberg, M. & Tilley, R. J. D. 1974 *J. Solid State Chem.* **11**, 150–160.
Tanisaki, S. 1960*a*. *J. Phys. Soc. Japan* **15**, 566–573.
Tanisaki, S. 1960*b* *J. Phys. Soc. Japan* **15**, 573–581.
Tilley, R. J. D. 1972 *M.T.P. Int. Rev. Sci., Inorg. Chem., Series* 1, **10** (ed. L. E. J. Roberts), pp. 279–313. London: Butterworths.
Tilley, R. J. D. 1975 *M.T.P. Int. Rev. Sci., Inorg. Chem., Series* 2, **10** (ed. L. E. J. Roberts), pp. 73–110. London: Butterworths.
Tilley, R. J. D. 1976 *J. Solid State Chem.* **19**, 53–62.
Torrens, T. L. 1972 *Interatomic potentials*, p. 229. New York: Academic Press.

PHILOSOPHICAL TRANSACTIONS OF THE ROYAL SOCIETY A MATHEMATICAL, PHYSICAL & ENGINEERING SCIENCES

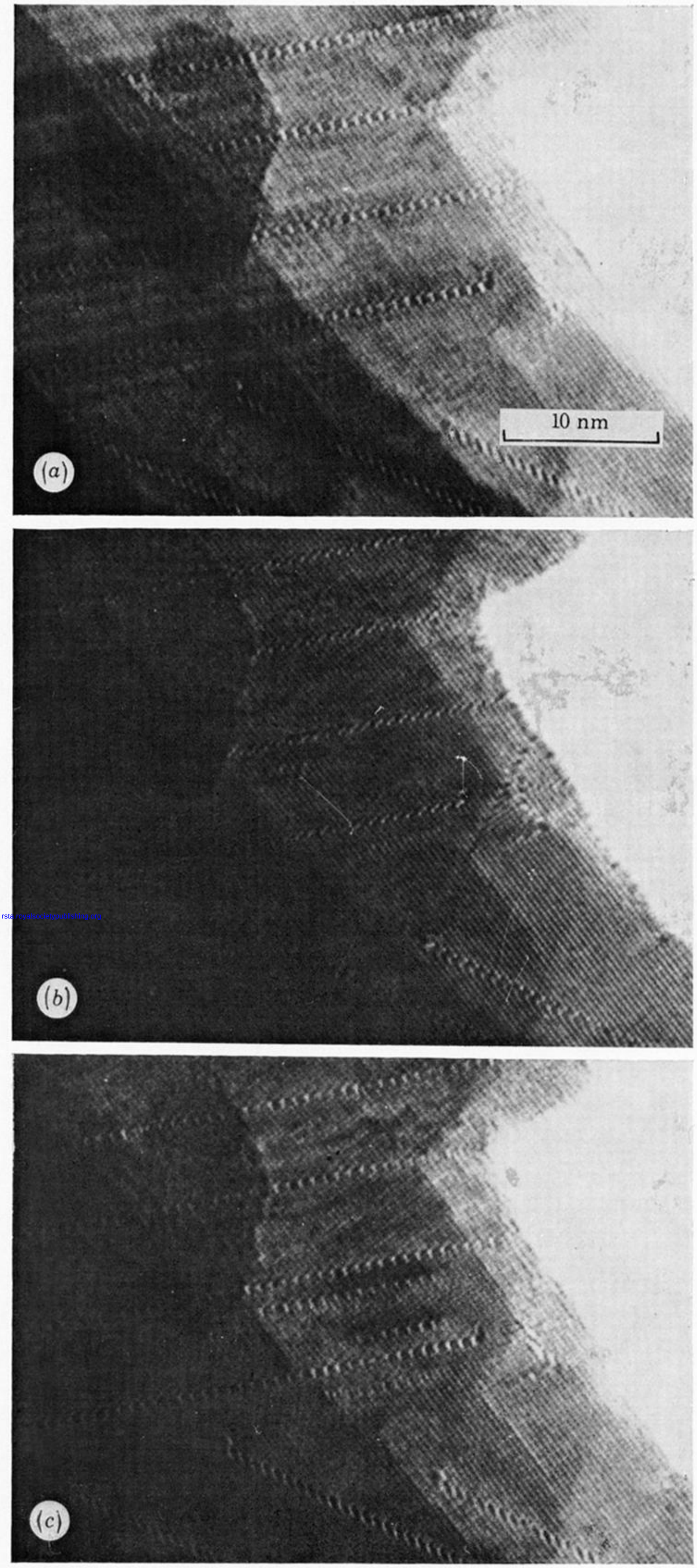

PHILOSOPHICAL TRANSACTIONS OF THE ROYAL SOCIETY A MATHEMATICAL, PHYSICAL & ENGINEERING SCIENCES

IGURE 12. (*a–c*) Electron micrographs showing the growth of pairs of {102} c.s. planes near to isolated {102} c.s. planes in slightly reduced WO_3; (*d*) a diagrammatic representation of the c.s. plane pairs formed in (*a–c*).

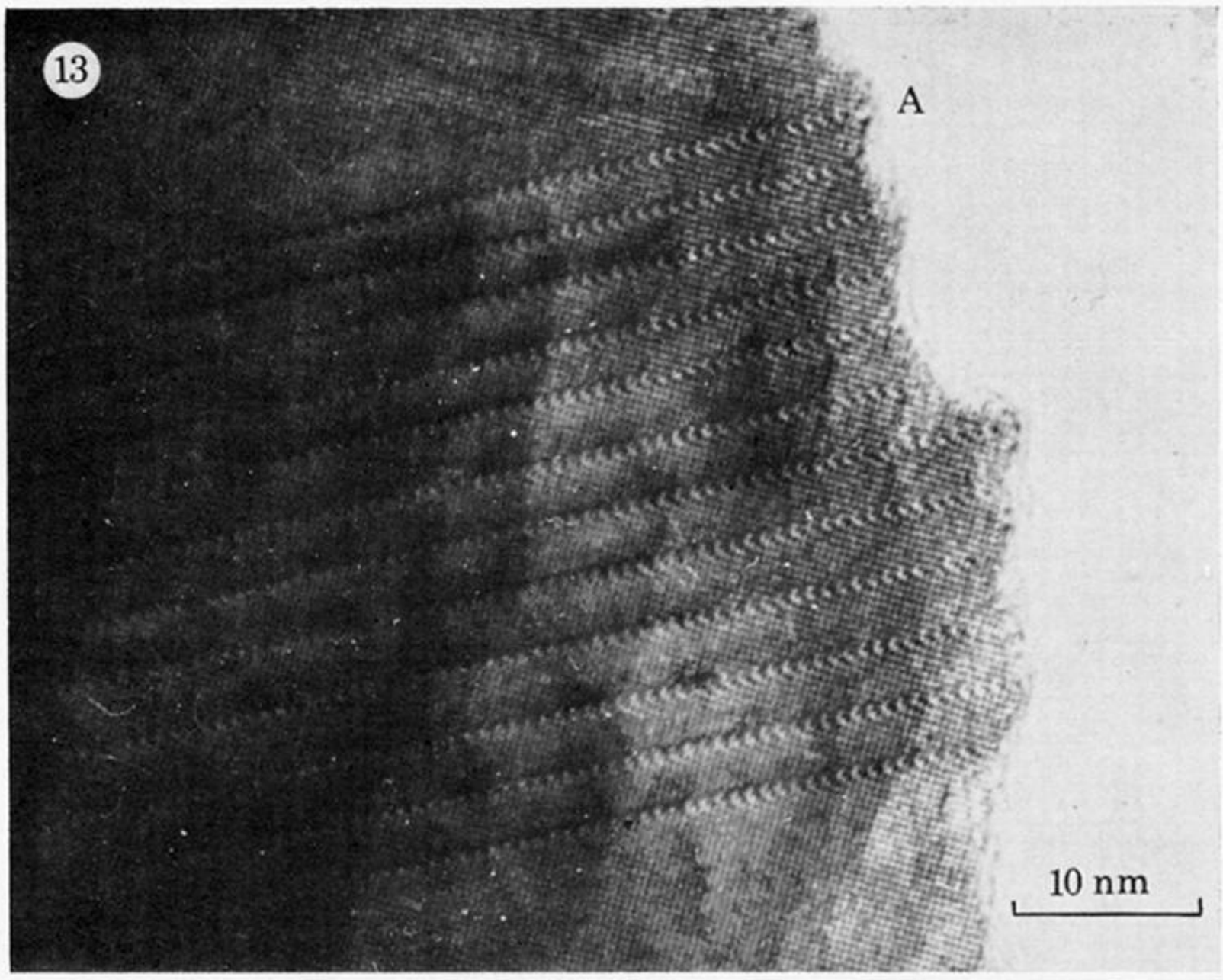

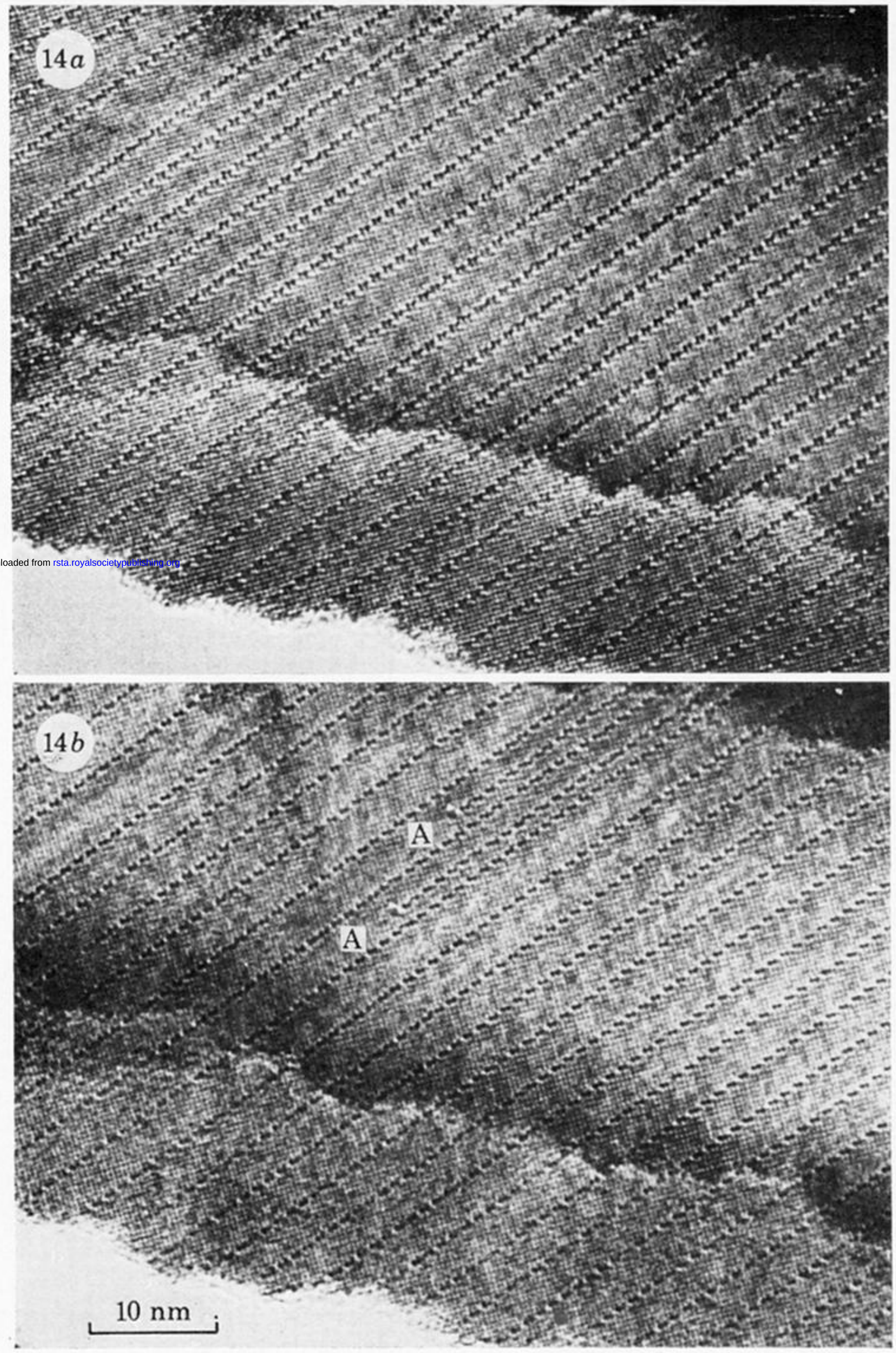

FIGURE 13. Electron micrograph of an isolated cluster of {102} c.s. planes in slightly reduced WO_3. The c.s. plane at A is in the process of growing into the crystal.

FIGURE 14 (*a*). Electron micrograph of a crystal containing quasi ordered {103} c.s. planes (*a*) before reduction in the electron microscope; (*b*) after observation, showing the growth of new c.s. planes, at A, A.